The Journal of Immunology

This information is current as of December 18, 2015.

A CpG-Ficoll Nanoparticle Adjuvant for Anthrax Protective Antigen Enhances Immunogenicity and Provides Single-Immunization Protection against Inhaled Anthrax in Monkeys

Melissa A. Kachura, Colin Hickle, Sariah A. Kell, Atul Sathe, Carlo Calacsan, Radwan Kiwan, Brian Hall, Robert Milley, Gary Ott, Robert L. Coffman, Holger Kanzler and John D. Campbell

Supplementary Material	http://www.jimmunol.org/content/suppl/2015/11/25/jimmunol.1501903.DCSupplemental.html
References	This article **cites 62 articles**, 23 of which you can access for free at: http://www.jimmunol.org/content/196/1/284.full#ref-list-1
Subscriptions	Information about subscribing to *The Journal of Immunology* is online at: http://jimmunol.org/subscriptions
Permissions	Submit copyright permission requests at: http://www.aai.org/ji/copyright.html
Email Alerts	Receive free email-alerts when new articles cite this article. Sign up at: http://jimmunol.org/cgi/alerts/etoc

A CpG-Ficoll Nanoparticle Adjuvant for Anthrax Protective Antigen Enhances Immunogenicity and Provides Single-Immunization Protection against Inhaled Anthrax in Monkeys

Melissa A. Kachura,* Colin Hickle,* Sariah A. Kell,* Atul Sathe,* Carlo Calacsan,* Radwan Kiwan,* Brian Hall,[†] Robert Milley,* Gary Ott,* Robert L. Coffman,[*,1] Holger Kanzler,[*,1,2] and John D. Campbell*

Nanoparticulate delivery systems for vaccine adjuvants, designed to enhance targeting of secondary lymphoid organs and activation of APCs, have shown substantial promise for enhanced immunopotentiation. We investigated the adjuvant activity of synthetic oligonucleotides containing CpG-rich motifs linked to the sucrose polymer Ficoll, forming soluble 50-nm particles (DV230-Ficoll), each containing >100 molecules of the TLR9 ligand, DV230. DV230-Ficoll was evaluated as an adjuvant for a candidate vaccine for anthrax using recombinant protective Ag (rPA) from *Bacillus anthracis*. A single immunization with rPA plus DV230-Ficoll induced 10-fold higher titers of toxin-neutralizing Abs in cynomolgus monkeys at 2 wk compared with animals immunized with equivalent amounts of monomeric DV230. Monkeys immunized either once or twice with rPA plus DV230-Ficoll were completely protected from challenge with 200 LD_{50} aerosolized anthrax spores. In mice, DV230-Ficoll was more potent than DV230 for the induction of innate immune responses at the injection site and draining lymph nodes. DV230-Ficoll was preferentially colocalized with rPA in key APC populations and induced greater maturation marker expression (CD69 and CD86) on these cells and stronger germinal center B and T cell responses, relative to DV230. DV230-Ficoll was also preferentially retained at the injection site and draining lymph nodes and produced fewer systemic inflammatory responses. These findings support the development of DV230-Ficoll as an adjuvant platform, particularly for vaccines such as for anthrax, for which rapid induction of protective immunity and memory with a single injection is very important. *The Journal of Immunology*, 2016, 196: 284–297.

Synthetic CpG motif–containing oligodeoxynucleotides (CpG-ODN) signal through TLR9 expressed in plasmacytoid dendritic cells (pDCs) and B cells and have potent adjuvant activity, promoting DC Ag presentation and inducing B cell differentiation into Ab-secreting cells (1, 2). The CpG-containing sequence 1018 is currently in late stage clinical development as an adjuvant for immunization against hepatitis B surface Ag (HBsAg) and demonstrates markedly improved efficacy over a currently licensed hepatitis B virus vaccine, Engerix-B (HBsAg absorbed to aluminum hydroxide [alum]) (3). In healthy individuals, two immunizations with HBsAg plus 1018 at 0 and 4 wk induced seroprotective Ab titer levels in 95% of vaccinated individuals by 8 wk after the second immunization, whereas the alum-adjuvanted vaccine required a three-immunization regimen spread over 6 mo to achieve 80% seroprotection (4). Additionally, HBsAg plus 1018 was significantly more effective at inducing protective titers in older adults and in immunocompromised populations such as patients with diabetes and those with chronic kidney disease (5, 6). Thus, in the context of hepatitis B vaccination, a CpG-ODN adjuvant has demonstrated significant advantages over alum.

In certain situations, such as pandemic infectious diseases or widespread exposure to biological warfare agents, vaccines providing rapid, single-immunization protection would be very advantageous. Given the demonstrated improvement over alum, CpG-ODN–based adjuvants are good candidates for optimization to further enhance rapidity and potency.

A particularly promising approach is incorporation of TLR agonists into nanoparticle form for coadministration with Ag. Nanoparticle formulations offer the potential of packaging adjuvant and/or Ags in particle sizes optimized for prolonged retention in draining lymph nodes and for enhanced uptake by APCs (7–9). CpG-ODN adjuvants have been evaluated in a variety of particulate formulations to enhance their adjuvant activity (10–12). We have previously shown that conjugating CpG-ODN molecules to the cross-linked

*Dynavax Technologies, Berkeley, CA 94710; and [†]Amnis Corp., EMD Millipore, Seattle, WA 98119

[1]R.L.C. and H.K. contributed equally to this work.

[2]Current address: MedImmune, Gaithersburg, MD.

ORCIDs: 0000-0001-5524-2523 (C.H.); 0000-0002-8526-3330 (J.D.C.).

Address correspondence and reprint requests to Robert L. Coffman and John D. Campbell, Dynavax Technologies, 2929 Seventh Street, Suite 100, Berkeley, CA 94710. E-mail addresses: RCoffman@dynavax.com (R.L.C.) and DCampbell@dynavax.com (J.D.C.)

The online version of this article contains supplemental material.

Abbreviations used in this article: AECM, *N*-(2-aminoethyl)carbamylmethyl; alum, aluminum hydroxide; AVA, anthrax vaccine adsorbed; BDS, bright detail similarity; cDC, conventional DC; DC, dendritic cell; DPBS, Dulbecco's PBS; GC, germinal center; HBsAg, hepatitis B surface Ag; HEG, hexaethylene glycol; IRG, IFN-regulated gene; LLOQ, lower limit of quantitation; mDC, myeloid DC; MHC II, MHC class II; NHP, nonhuman primate; ODN, oligodeoxynucleotide; pDC, plasmacytoid dendritic cell; PNA, peanut agglutinin; rPA, recombinant protective Ag; SM-PEG₆, succinimidyl-([*N*-maleimidopropionamidyl]-hexethyleneglycol)ester; T_{FH}, T follicular helper; TNA, toxin-neutralizing Ab.

sucrose polymer Ficoll augments IFN-α production from human pDCs in vitro compared with cells stimulated with nonconjugated CpG-ODN molecules (13, 14). Ficoll has a large number of available reactive sites for conjugation to CpG-ODN molecules, can be engineered to form nanoparticles of consistent size distribution, is considered nonimmunogenic, and has generated no toxicity signals in limited clinical studies (15, 16).

To determine whether a CpG-Ficoll nanoparticle formulation would improve adjuvant activity in vivo, we conjugated the CpG-containing ODN, DV230, to Ficoll, generating particles with a median size of 50 nm, containing ~120 DV230 molecules. The relative adjuvant activity of DV230-Ficoll nanoparticles was compared with monomeric DV230 for potency and rapidity of induction of Ab responses to recombinant protective Ag (rPA) from the Gram-positive, spore-forming bacterium *Bacillus anthracis*, the causative agent of anthrax. *B. anthracis* is classified by the Centers for Disease Control as a category A agent due to the potential high lethality of a possible bioterrorism-related exposure incident. The current regimen for administration of anthrax vaccine absorbed (AVA; BioThrax), the U.S.-licensed vaccine, requires three immunizations administered over 6 mo, followed by booster shots at 12 and 18 mo (17). Efficacy of immunization regimens with rPA can be evaluated by measurement of toxin-neutralizing Ab (TNA) levels, which are regarded as a correlate of protection (18, 19). In this study, we evaluated the relative ability of DV230-Ficoll nanoparticles and monomeric DV230 to adjuvant anti-rPA Ab responses in cynomolgus macaques, and tested the ability of one and two

DV230-Ficoll immunization regimens to protect monkeys from lethal aerosol challenge with anthrax spores. Differences in the mechanism of action in vivo of the nanoparticle and monomeric adjuvants were evaluated in mice. In this study, we report protection from lethal anthrax aerosol challenge in primates following a single-immunization regimen. The data further demonstrate augmented uptake and activation of innate immune cells in response to DV230-Ficoll as well as prolonged retention of the nanoparticle adjuvant at the injection site and draining lymph nodes. These findings support further development of a Ficoll-based platform for enhancement of adjuvant potency in vivo.

Materials and Methods

Reagents

The CpG ODN DV230, composed of phosphorothioate 7-mers, connected with inert, hexaethylene glycol (HEG) spacers and with the specific sequence 5′-TCGGCGC-HEG-AACGTTC-HEG-TCGGCGC-3′, was synthesized and HPLC purified by Avecia (Milford, MA). DV230-Ficoll was synthesized by a modified version of the method of Inman (20). Briefly, N-(2-aminoethyl)carbamylmethyl (AECM)–Ficoll as first synthesized by acetylation of Ficoll with chloroacetic acid, was followed by reaction with excess ethylene diamine and 1-ethyl-3-(3-dimethylaminopropyl)carbodiimide. AECM-Ficoll was activated by reaction with the amino-reactive heterobifunctional crosslinker succinimidyl-([N-maleimidopropionamidyl]hexethyleneglycol)ester (SM-PEG$_6$) to form a sulfhydryl-reactive Ficoll derivative. The activated SM-PEG$_6$–Ficoll was then reacted with a 3′-thiol derivative of DV230 (DV230-SH) to yield the DV230-Ficoll product. For fluorescently labeled DV230-Ficoll, AECM-Ficoll was reacted with Alexa Fluor 555–NHS
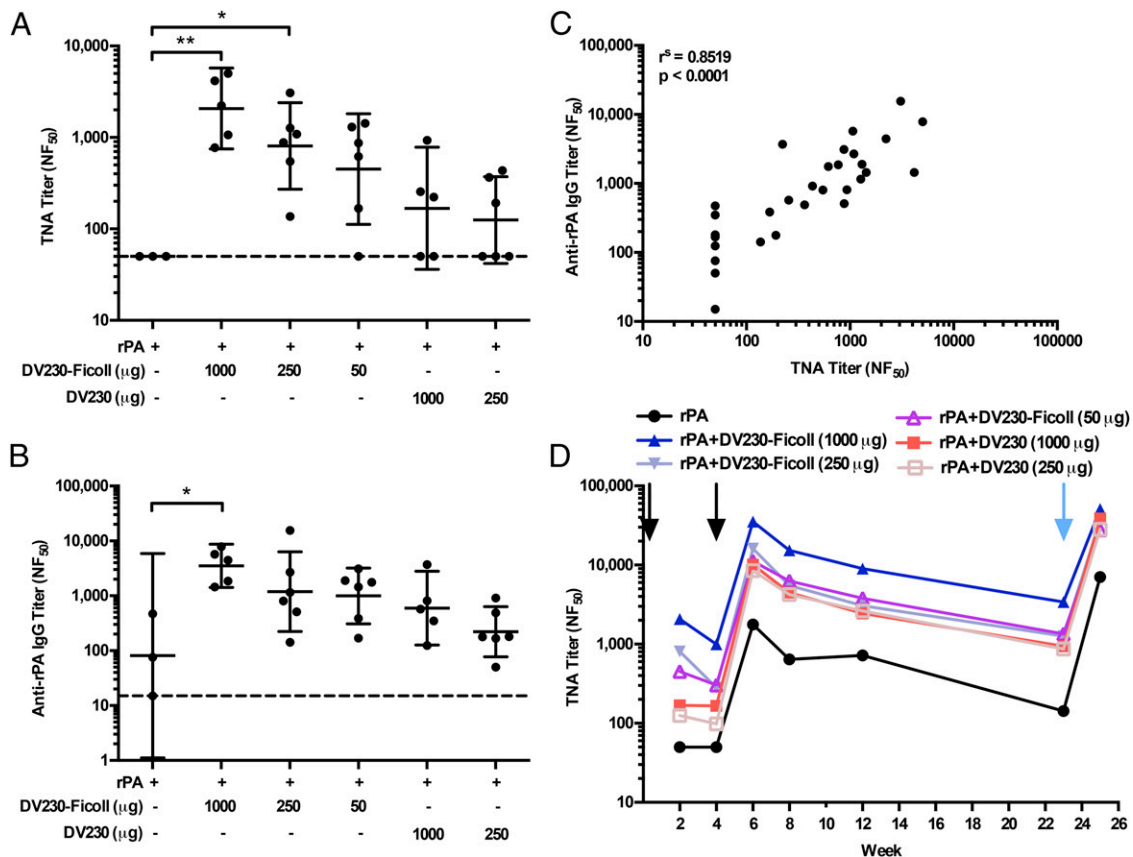
FIGURE 1. rPA/DV230-Ficoll vaccination leads to rapid induction of anti-rPA Ab response and long-lasting memory in monkeys. Cynomolgus macaques (*n* = 3–6/group) were immunized i.m. (black ↓) with 10 μg rPA alone or in combination with 1000, 250, or 50 μg DV230-Ficoll or 1000 or 250 μg DV230 on days 0 and 28. All monkeys received 25 μg rPA alone (blue ↓) 23 wk following initial immunization. TNA and anti-rPA IgG titer levels were monitored for 25 wk following initial immunization. (**A** and **B**) Titers 2 wk following initial immunization are shown as mean with 95% CI; data shown are representative of three independent experiments. *$p < 0.05$, ** $p < 0.01$ by Kruskal–Wallis with Dunn posttest. (**C**) Correlation between anti-rPA IgG and TNA titer levels 2 wk following initial immunization. Spearman rank correlation. (**D**) TNA titer data monitored throughout the study are shown as means.

ester (Life Technologies, Foster City, CA) and SM-PEG$_6$ to form maleimide/ Alexa Fluor 555–Ficoll, which was further reacted with DV230-SH, as described above, to yield the Alexa Fluor 555/DV230-Ficoll product with a resulting ratio of one Alexa Fluor 555 per four DV230. Alexa Fluor 647– NHS ester (Life Technologies) was reacted with rPA to yield Alexa Fluor 647/rPA with a resulting ratio of one Alexa Fluor 647 per rPA. Alexa Fluor 555/DV230 was synthesized by TriLink BioTechnologies (San Diego, CA) containing one Alexa Fluor 555 per DV230. The rPA protein was provided by PharmAthene (Annapolis, MD).

Animals

Cynomolgus monkeys (*Macaca fascicularis*) were housed at Valley Bio-systems (West Sacramento, CA) or at Battelle Biomedical Research Center (Columbus, OH). Only healthy adult animals were used in each study. Swiss Webster, BALB/c, and C57BL/6 mice, purchased from Charles River Laboratories (Hollister, CA) and used at 8–12 wk of age, were maintained at Pacific BioLabs (Hercules, CA) or MuriGenics (Vallejo, CA). TLR9$^{-/-}$ mice (21) were maintained at Simonsen Laboratories (Gilroy, CA) and used at 8–16 wk of age. All animal studies were com-pliant with the U.S. Department of Health and Human Services *Guide for the Care and Use of Laboratory Animals* and were approved by the In-stitutional Animal Care and Use Committees of the respective facilities.

Nonhuman primate immunogenicity and anthrax challenge studies

For immunogenicity studies, groups of cynomolgus monkeys were im-munized by either the i.m. (quadriceps) or s.c. route with rPA with/without doses of DV230 or DV230-Ficoll in a total volume of 1 ml Dulbecco's PBS (DPBS; BioWhittaker, Walkersville, MD) with subsequent blood draws to assess effects of adjuvants on Ab responses. For the anthrax aerosol challenge study, 25 male and 25 female cynomolgus monkeys were ran-domized by weight into groups of eight (four male, four female) or six (three male, three female). Animals were immunized by the i.m. route (quadriceps) on days 0 and/or 29 with 10 μg rPA with/without 1000 or 250 μg DV230-Ficoll or DV230 in a total volume of 1 ml DPBS. A group of six nonimmunized animals was also included. Monkeys in the non-immunized and rPA/DV230-Ficoll immunized groups were exposed to a target dose of 200 LD$_{50}$ equivalents of aerosolized *B. anthracis* Ames spores on day 69, 70, or 71 (delivered dose was 252 ± 50 [mean ± SD] LD$_{50}$). Monkeys were randomized to one of the three challenge days, with at least two monkeys from each group assigned to each day. The animals were monitored twice daily for survival and clinical signs of illness for 28 d following challenge. Any animal judged to be moribund was im-mediately euthanized. If possible, postexposure blood and/or serum

FIGURE 2. rPA/DV230-Ficoll vaccination induces a potent memory response, mediating complete pro-tection from challenge with aerosolized *B. anthracis* spores in a monkey prophylactic anthrax challenge model. (**A** and **B**) Cynomolgus macaques (*n* = 6–8/ group) were immunized i.m. (black ↓) with 10 μg rPA in combination with 1000 or 250 μg DV230-Ficoll on day 0 and/or 29 (1× or 2×). A group (*n* = 6) of non-vaccinated animals was also included. All monkeys were exposed to a target dose of 200 LD$_{50}$ equivalents of aerosolized *B. anthracis* spores on day 69, 70, or 71 (red ↓). (A) Survival was monitored twice daily for 28 d following challenge. (B) TNA titer levels were moni-tored throughout the study and for 4 wk following challenge. Data are shown as mean with 95% CI. Data are from a single experiment. (**C**) Cynomolgus ma-caques (*n* = 4–6) were immunized with 10 μg rPA alone or in combination with 1000, 50, 20, or 5 μg DV230-Ficoll on days 0 and 28 (black ↓). All monkeys received 25 μg rPA alone 10 wk following initial im-munization (blue ↓). TNA titer levels were monitored for 12 wk. Titers are shown as means. Data are from a single experiment.
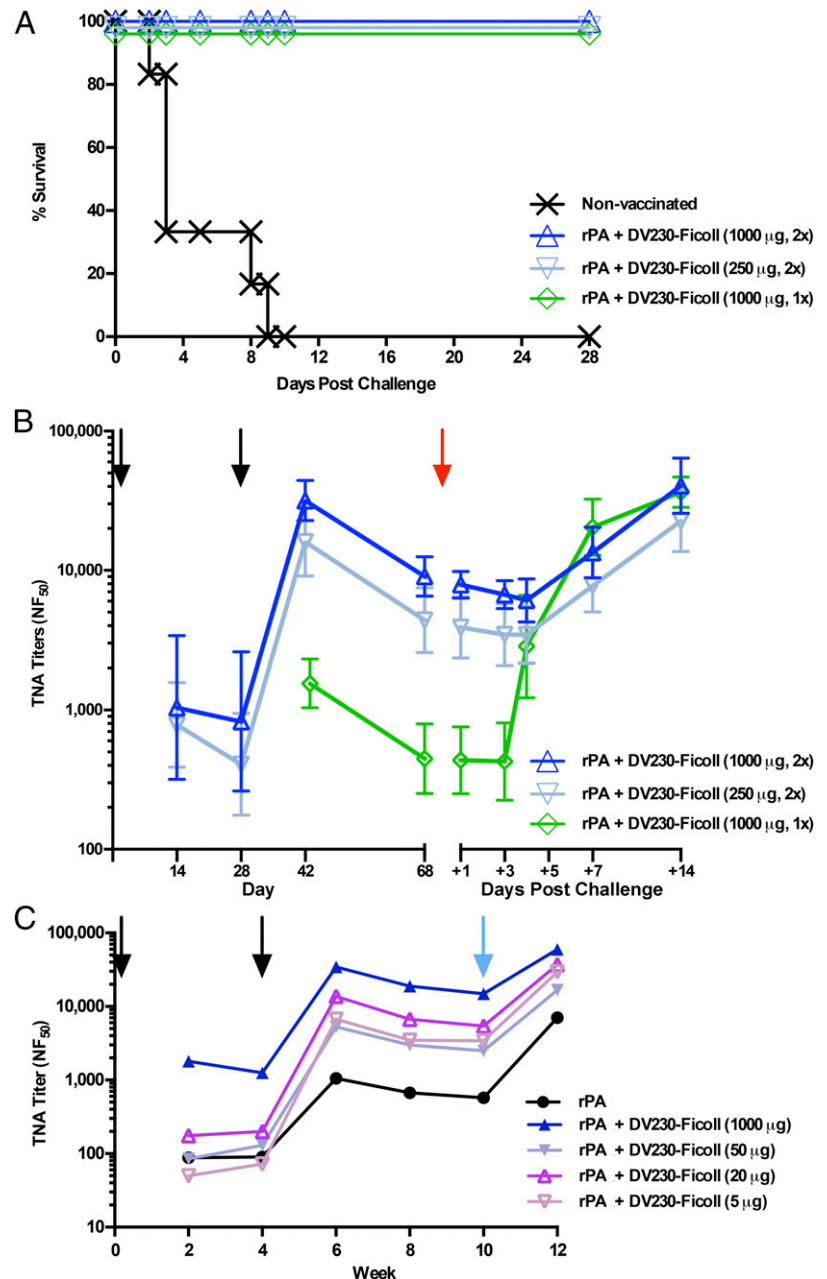
samples were collected. Qualitative bacteremia was assessed from day 62 onward by streaking 30–40 μl EDTA whole blood onto blood agar plates and incubating at 37°C for at least 48 h. Samples resulting in any colonies consistent with *B. anthracis* morphology (γ-hemolytic, white colonies, 4–10 mm in diameter with a rough appearance and irregular edges) were documented as positive.

Mouse studies

For immunogenicity, tissue distribution, and systemic toxicity studies, mice were injected in the quadriceps with adjuvant with/without rPA, or with rPA alone. For studies assessing muscle tissue responses, mice were injected bilaterally in the quadriceps with adjuvant alone. For draining lymph node responses, including gene expression and flow cytometry assessments, mice were injected in both rear footpads with adjuvant with/without rPA. DV230–Alexa Fluor 555, when used, was administered in combination with non-labeled DV230 in a ratio to match Alexa Fluor 555/DV230-Ficoll–specific relative fluorescence. All immunizations were performed in a total volume of 50 μl DPBS or 10 mM sodium phosphate buffer.

Serological assays

Toxin-neutralizing Ab. TNA titers were measured as previously described (22). Titers were calculated as the reciprocal of the dilution of the serum sample producing 50% neutralization of toxin-mediated cytotoxicity (ED_{50}) corresponding to the inflection point of a four-parameter logistic log fit of the neutralization curve. Results are reported as the quotient of the ED_{50} of the test sample and the ED_{50} of a reference standard (NF_{50}). Human reference standard AVR801 was used for standardization. Data acquisition and analysis were performed by a SpectraMax 190 or VersaMax using SoftMaxPro version 5.0.1 (Molecular Devices, Sunnyvale, CA) or SAS (SAS Institute, Cary, NC). The lower limit of quantitation (LLOQ) was 100. Samples resulting in undetectable values were assigned a value equal to half the LLOQ.

Anti-rPA IgG quantification. Plates (96 well) were coated with rPA and incubated overnight. Standards and test sera, at appropriate dilution series, were assayed in duplicate. HRP-conjugated goat anti-human IgG (SouthernBiotech, Birmingham, AL) was used for detection and color was developed with a 3,3′,5,5′-tetramethylbenzidine Microwell Peroxidase Substrate System (KPL, Gaithersburg, MD). Titers were calculated as the reciprocal of the dilution (ED_{50}), corresponding to the inflection point of a four-parameter logistic log fit curve. Results are reported as the quotient of the ED_{50} of the test sample and the ED_{50} of a reference standard (NF_{50}). Data acquisition and analysis were performed by a SpectraMax 190 or VersaMax using SoftMaxPro v5.0.1 software (Molecular Devices).

Cytokine quantification. Mouse TNF-α (R&D Systems, Minneapolis, MN), IL-6 (BD Pharmingen, San Diego, CA), and IL-12p40 (BD Pharmingen) were assayed per the manufacturers' recommendations. LLOQs were 156, 78, and 46 pg/ml, respectively. Data acquisition and analysis were performed by a SpectraMax 190 or VersaMax using SoftMaxPro v5.0.1 software (Molecular Devices).

Quantitative real-time RT-PCR

Organs were frozen in RNAlater (Qiagen, Venlo, The Netherlands). Total RNA was isolated from 30 mg per individual homogenized muscle using an RNeasy fibrous tissue mini kit (Qiagen) and entire homogenized popliteal lymph node using an RNeasy mini kit (Qiagen), both with on-column DNase I digestion. RNA was reverse transcribed using recombinant RNasin RNase inhibitor (Promega, Madison, WI), oligo(dT)$_{15}$ (Promega), random primers (Promega), dNTP (Invitrogen, Carlsbad, CA), and SuperScript III reverse transcriptase (Invitrogen). Quantification of mRNA was performed using Power SYBR Green master mix (Life Technologies), with cycling conditions of 15 min at 95°C, followed by 40 rounds of 15 s at 95°C and 1 min at 60°C, with data normalized to ubiquitin expression. Sequence information for primers used is listed in Supplemental Table I. Alternately, RNA was reverse transcribed by an RT^2 First Strand Kit (Qiagen) for use with the RT^2 Profiler PCR array system (Qiagen) for cytokines and chemokines according to the manufacturer's directions. All quantification and analysis were performed using an Applied Biosystems (Carlsbad, CA) StepOnePlus real-time PCR system using StepOne v2.1 software.

Flow cytometry

Single-cell suspensions were prepared from mouse tissues and pooled by experimental group as previously described (23), excepting muscle, which was first digested with 2 mg/ml collagenase, type 2 (Worthington Biochemical, Lakewood, NJ) for 45 min at 37°C. Cells were stained for 30 min at 4°C in DPBS containing 0.1% BSA with/without 2 mM EDTA after

blocking FcγR with clone 2.4G2 mAb. Cells were fixed in a final concentration of 1% formaldehyde for a minimum of 20 min, followed by washing and resuspension in FACS flow buffer. Abs against CD3ε (145-2C11), CD4 (GK1.5), CD8α (53-6.7), CD11b (M1/70), CD11c (HL3), CD19 (6D5), CD45R/B220 (RA3-6B2), CD49b (DX5), CD69 (H1.2F3), CD86 (GL-1), CD95 (Jo2), CD279 (J43), CD317/PDCA-1 (eBio927), CXCR5 (2G8), F4/80 (BM8), Ly-6C (AL-21), Ly-6G (1A8), MHC class II (MHC II; I-A/I-E) (M5/114.15.2), and T and B Cell activation Ag (GL7) were purchased from BD Biosciences (San Jose, CA), BioLegend (San Diego, CA), or eBioscience (San Diego, CA). Biotinylated peanut agglutinin (PNA) was purchased from Vector Laboratories (Burlingame, CA). Flow cytometry data were collected on an LSR II (BD Biosciences) flow cytometer and analyzed using FlowJo software (Tree Star, Ashland, OR). A representative flow cytometry gating strategy for non–germinal center (GC) cell populations is shown in Supplemental Fig. 1. Polychromatic imaging flow cytometry data were collected on an ImageStream^X mk II (Amnis, Seattle, WA) and analyzed using IDEAS v6.1 software as previously described (24). Images were captured using a ×60 lens with a 0.9 numerical aperture and 2.5-μm effective depth of field. Cells likely to have colocalized fluorescent signals were identified with aid of bright detail similarity (BDS). BDS scoring quantifies colocalization between fluorescent markers within cells by comparing the spatial location and degree of overlap to calculate the non–mean-normalized Pearson correlation coefficient of the images (24). Events with BDS scores over the threshold level of 2 were likely to have fluorescence colocalization, which was confirmed visually.

DV230-Ficoll or DV230 tissue quantification by enzyme-linked hybridization assay or hybridization assay

Spleen, liver, kidney, or injection site muscle, 25–50 mg per tissue per individual animal, and draining lymph nodes, pooled per individual animal, were
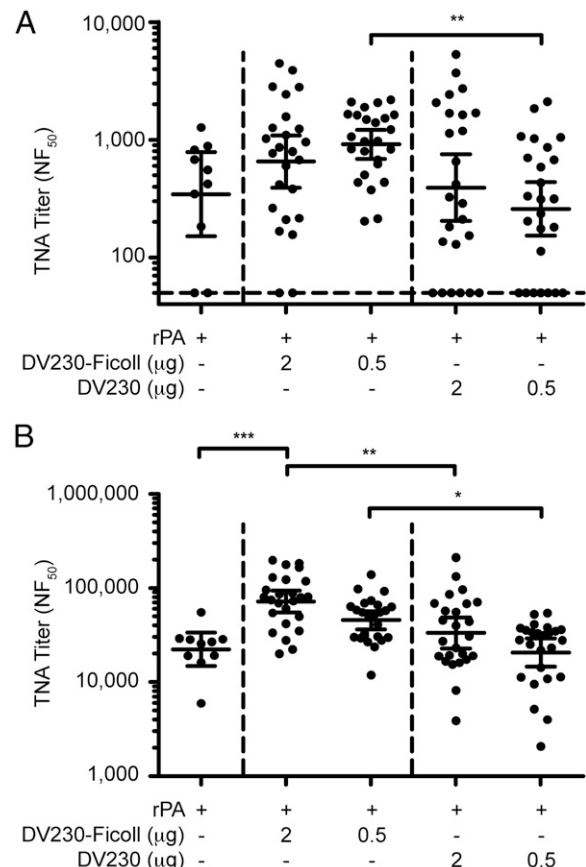
FIGURE 3. rPA/DV230-Ficoll immunization induces greater primary and secondary TNA titer responses in mice. Swiss Webster mice (*n* = 25/ group) were immunized with 5 μg rPA alone or in combination with 2 or 0.5 μg DV230-Ficoll or DV230 on days 0 and 29. TNA titer levels were assessed (**A**) 4 wk after the first immunization and (**B**) 2 wk after the second immunization. Data are shown as means with 95% CI. *$p < 0.05$, **$p < 0.01$, ***$p < 0.001$ by Kruskal–Wallis with a Dunn posttest. Data are from a single experiment.

homogenized in 20 mM Tris (pH 8), 20 mM EDTA (Sigma-Aldrich, St. Louis, MO), 100 mM sodium chloride, 0.2% SDS (Teknova, Hollister, CA) using the TissueLyser II (Qiagen), and subject to proteinase K (New England BioLabs, Ipswitch, MA) digestion at 1.2 U/mg tissue for 6–20 h at 50°C. Nunc Immobilizer amino plates were coated overnight at 4°C with 30 ng/ml capture probe (5′-GCGCCGAGAACGTTGCGCCGA-3′ for DV230 quantification; 5′-AGCCGCGTTGCAAGAGAAGCGATGCGCGGCTCG-3′ for DV230-Ficoll quantification) in 0.1 M sodium phosphate (Teknova). For quantification of DV230-Ficoll, homogenized samples, mixed in equal volume with 0.6 μg/ml detection probe (5′-GCGCCGAGAACGTTGCGCCGA-3′), were incubated for 75 min at 52°C. For quantification of DV230, homogenized samples, mixed in equal volume with SSC plus 2% N-lauroylsarcosine sodium salt buffer, were incubated for 2 h at 45°C and allowed to cool for 30 min at room temperature. Synthesis of complementary 3′ ends of captured DV230 was catalyzed by 1.25 U Klenow fragment (New England BioLabs) in the presence of 0.5 μM biotinylated dUTP and 50 μM dNTP (New England BioLabs). HRP-conjugated streptavidin (Thermo Scientific, Waltham, MA) was used for adjuvant detection, and color was developed with a 3,3′,5,5′-tetramethylbenzidine microwell peroxidase substrate system (KPL). Adjuvants served as standards. The LLOQs were 6.24 and 7.62 ng/g tissue for DV230-Ficoll and DV230, respectively. All data acquisition and analysis were performed by a SpectraMax 190 or VersaMax using Soft-MaxPro v5.0.1 software (Molecular Devices).

Statistical analysis

A Mann–Whitney or Kruskal–Wallis test with a Dunn posttest, as specified in the figure legends, was used to determine statistical significance. A p value ≤0.05 was considered significant.

Results

rPA/DV230-Ficoll immunization induces a rapid primary immune response, long-lasting memory, and protection from lethal anthrax aerosol challenge in monkeys

To definitively compare the activity of DV230-Ficoll nanoparticles to monomeric DV230, we tested the relative ability of each adjuvant to enhance Ab responses against rPA in cynomolgus monkeys. Monkeys were chosen because cellular expression patterns for TLR9 are similar between humans and nonhuman primates (NHPs), whereas TLR9 distribution and TLR9-mediated responses are

FIGURE 4. DV230-Ficoll nanoparticles, compared with monomeric DV230, enhance expression of IFN-regulated, chemokine, cytokine, and transendothelial migration–related genes, leading to enhanced cell recruitment in injection site muscle. BALB/c mice (n = 6/group) were injected i.m. with 10 μg DV230-Ficoll or DV230 (CpG-ODN–based doses). Injection site muscle was collected 6 h following injection to assess (**A**) IFN-regulated, (**B**) chemokine, (**C**) cytokine, and (**D**) transendothelial migration–related gene expression. Gene expression relative to PBS-injected controls was determined by ΔΔCt evaluation ($2^{-\Delta\Delta Ct}$). Data are shown as mean of individual samples with 95% CI. Data are from a single experiment. (**E**) Relative proportions of various cell populations in muscle (normalized to total cells) of DV230-Ficoll– versus DV230-injected mice (10 μg) at 12–24 h were evaluated by flow cytometry. Following light scatter gating and exclusion of lymphocytes (CD3/CD19/CD49b dump channel), cell populations were identified as follows: macrophages (CD11b⁺/CD11c⁻/F4/80⁺/Ly6C⁺/Ly6G⁻), monocytes (CD11b⁺/CD11c⁻/F4/80⁻/Ly6C⁺/Ly6G⁻), neutrophils (CD11b⁺/CD11c⁻/Ly6G⁺), total CD11b⁺ cells, and cDCs (CD11b⁻/CD11c⁺). Data shown as means with SEM are an average of two independent experiments.
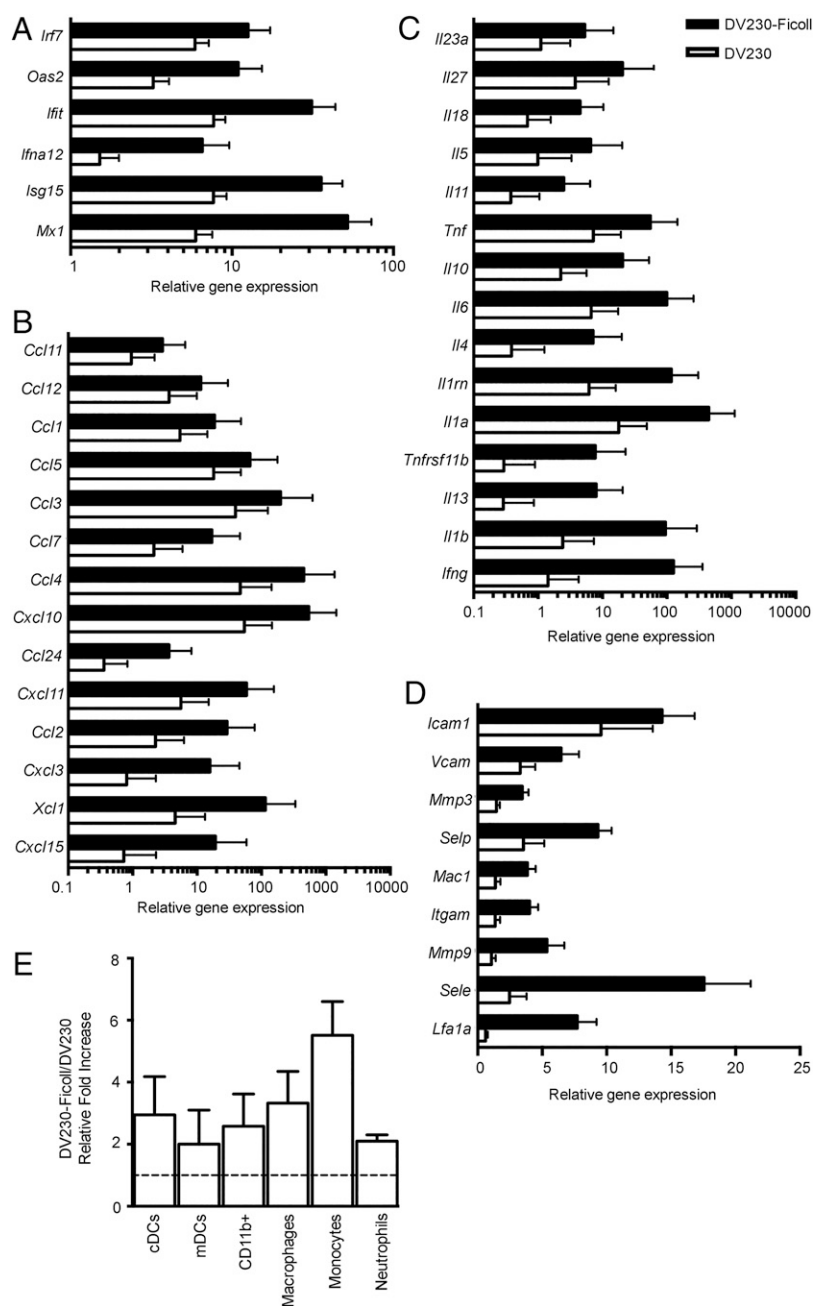
quite different in rodents (25, 26). Additionally, the pathology and clinical progression of inhalational anthrax in NHPs is comparable to humans, supporting the use of monkeys to evaluate protection by anthrax vaccine candidates (27, 28). Groups of monkeys were immunized i.m. with rPA combined with either DV230-Ficoll or DV230 at equivalent CpG-based doses on days 0 and 28. Serum TNA titers, a well-defined correlate of protection against anthrax challenge (19), were monitored. As early as 14 d following a primary immunization, rPA/DV230-Ficoll induced higher TNA titers compared with rPA/DV230 at all doses (Fig. 1A). The two highest doses of DV230-Ficoll induced mean TNA titers that were significantly higher than in animals given only rPA, compared with a nonsignificant increase by DV230 addition. At the highest dose of DV230-Ficoll, the calculated 31-fold increase in TNA titers compared with rPA alone is likely an underestimate of the adjuvant potency, as titers in rPA only animals were all below the level of detection for the TNA assay. Additionally, all animals (11 of 11) receiving 250–1000 μg DV230-Ficoll were seropositive whereas 5 of 11 animals immunized with 250–1000 μg DV230 were below the LLOQ. Likewise, titers of total anti-rPA IgG at 14 d were significantly increased following immunization with rPA/DV230-Ficoll (Fig. 1B) and were significantly correlated to the TNA results (Fig. 1C). Following the second immunization at day 28, a >15-fold boost in TNA responses was evident in all groups and the titers remained elevated for at least 18 wk. The memory response to antigenic challenge ∼5 mo following a second immunization was also evaluated in these animals. Further increases in TNA titers of at least 15-fold (Fig. 1D) demonstrated a rapid, robust response, indicating potentially protective immunity.

The TNA titers achieved even after a single injection of rPA plus DV230-Ficoll compared favorably with titers correlated with protection against live anthrax challenge in cynomolgus monkeys (19). To directly evaluate protection, cynomolgus macaques were immunized i.m. with rPA plus DV230-Ficoll once (day 29) or twice (days 0 and 29) and challenged with a targeted dose of 200 LD_{50} equivalents of aerosolized *B. anthracis* spores on day 70 ± 1. Survival, bacteremia, and symptoms of clinical disease were monitored for 28 d following challenge and serum samples collected before and after challenge for determination of TNA titers.

Complete protection from anthrax challenge was achieved in all monkeys receiving a single vaccination of rPA with 1000 μg DV230-Ficoll or two vaccinations with either 250 or 1000 μg DV230-Ficoll, whereas all unvaccinated animals succumbed to disease within 9 d of challenge (Fig. 2A). Furthermore, no animals vaccinated with rPA/DV230-Ficoll showed bacteremia or clinical symptoms at any time point after challenge. Following challenge, all animals produced a rapid increase in TNA titers, indicating a strong memory response. The memory response was striking in monkeys receiving a single rPA/DV230-Ficoll immunization, rising rapidly to levels comparable to twice-immunized animals within 7 d of the infectious challenge (Fig. 2B). Taken together, these data demonstrate that a single immunization of rPA plus 1000 μg DV230-Ficoll primes animals for a prominent recall response and provides protection against lethal challenge with aerosolized *B. anthracis* spores.

Although rapid, single-injection protection against anthrax exposure represents an unmet need, the potent adjuvant activity of DV230-Ficoll suggested that substantially reduced doses may be effective in situations where a two-injection prophylactic regimen is feasible. Therefore, in a separate experiment, we monitored TNA responses in monkeys immunized on days 0 and 28 with rPA and DV230-Ficoll at 1000, 50, 20, or 5 μg. TNA titers >1000 were elicited in the two-immunization regimen, even with a DV230-Ficoll dose of 5 μg, the lowest dose tested, and were further boosted to >10,000 by Ag only injection (used as a surrogate for bacterial spore exposure) (Fig. 2C). Thus, in the context of a two-immunization regimen, the data suggest protective capacity with 1/200 of the DV230-Ficoll dose demonstrated to be protective in a single-immunization regimen in monkeys.

Enhanced immunogenicity of rPA/DV230-Ficoll is maintained in mice

The higher TNA titers achieved after immunization with rPA/DV230-Ficoll as compared with rPA/DV230 in monkeys suggests that DV230 delivered to the immune system in a virus-sized nanoparticle may facilitate more potent activation of early innate and adaptive immune responses to CpG-ODN. As the mouse is a more practical species for extensive mechanistic studies, we first

FIGURE 5. Adjuvant effects of DV230-Ficoll are dependent on TLR9 expression. (**A**) Wild-type (C57BL/6) or TLR9$^{-/-}$ mice (*n* = 6) were injected i.m. with 10 μg DV230-Ficoll. Injection site muscle was collected 6 h following injection to determine gene expression. Individual gene fold induction was calculated relative to PBS-injected controls. Data are shown as means with SEM. (**B**) C57BL/6 or TLR9$^{-/-}$ mice (*n* = 8–10) were immunized i.m. with 5 μg rPA in combination with 10 μg DV230-Ficoll. TNA titer levels at day 14 are shown as means. ***p* < 0.001 by Mann–Whitney *U* test. Data are from single experiments.
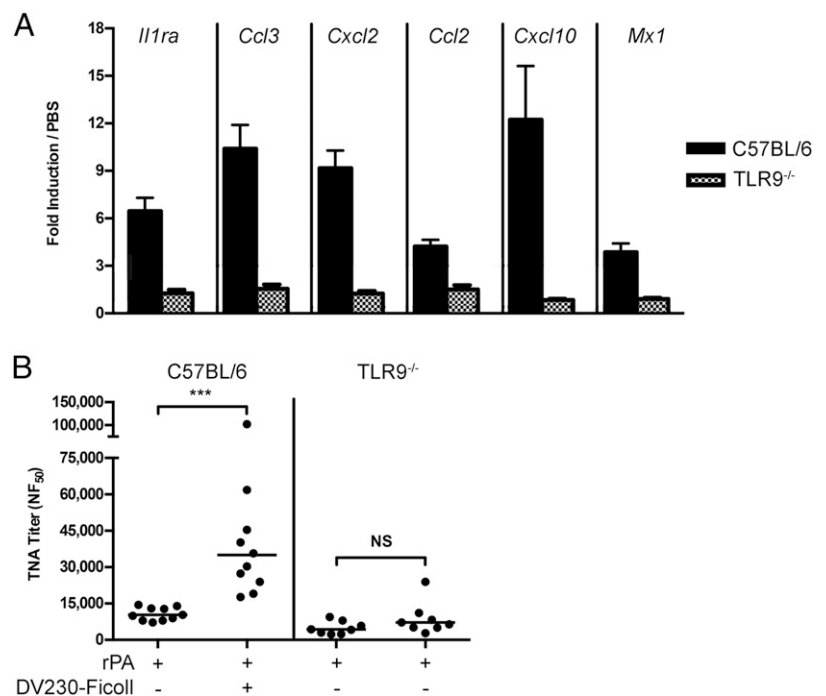
confirmed improved adjuvant activity by the DV230-Ficoll nanoparticle formulation in this species. Indeed, rPA/DV230-Ficoll induced significantly higher TNA titers after both a first and second immunization in mice, demonstrating the relevance of the species for studies investigating DV230-Ficoll mechanism of action (Fig. 3).

DV230-Ficoll nanoparticles preferentially enhance injection site gene expression and cellular infiltration

Ligation of TLR9 by CpG-containing ODN results in activation of the MyD88 pathway and signaling through IFN regulatory factor 7 and NF-κB for induction of IFN and inflammatory genes, respectively (29, 30). To assess early DV230-Ficoll effects in local tissue that may be associated with improved adjuvant activity compared with monomeric DV230, we analyzed transcriptional changes in injection site muscle 6 h after injection. Mice were

injected with adjuvants, without rPA, at equivalent CpG-based doses, with PBS-injected animals serving as controls. DV230-Ficoll exhibited a more potent effect on both the number of genes induced and the level of gene induction compared with the effect of monomeric DV230, both for multiple IFN-regulated genes (IRGs) (Fig. 4A) and chemokines (Fig. 4B). Likewise, DV230-Ficoll induced higher levels of cytokines of the IL-1 and TNF superfamilies (Fig. 4C). Adhesion molecules, integrins, and matrix metalloproteinases were also induced to a much greater degree in injection site muscle following DV230-Ficoll treatment (Fig. 4D). Thus, DV230 in a nanoparticle-like formulation is more efficient at inducing early markers of immune activation at the injection site compared with monomeric DV230. To determine whether nanoparticulate and monomeric DV230 differentially affected cellular recruitment to injection site muscle, relative proportions of immune cell populations were analyzed by flow
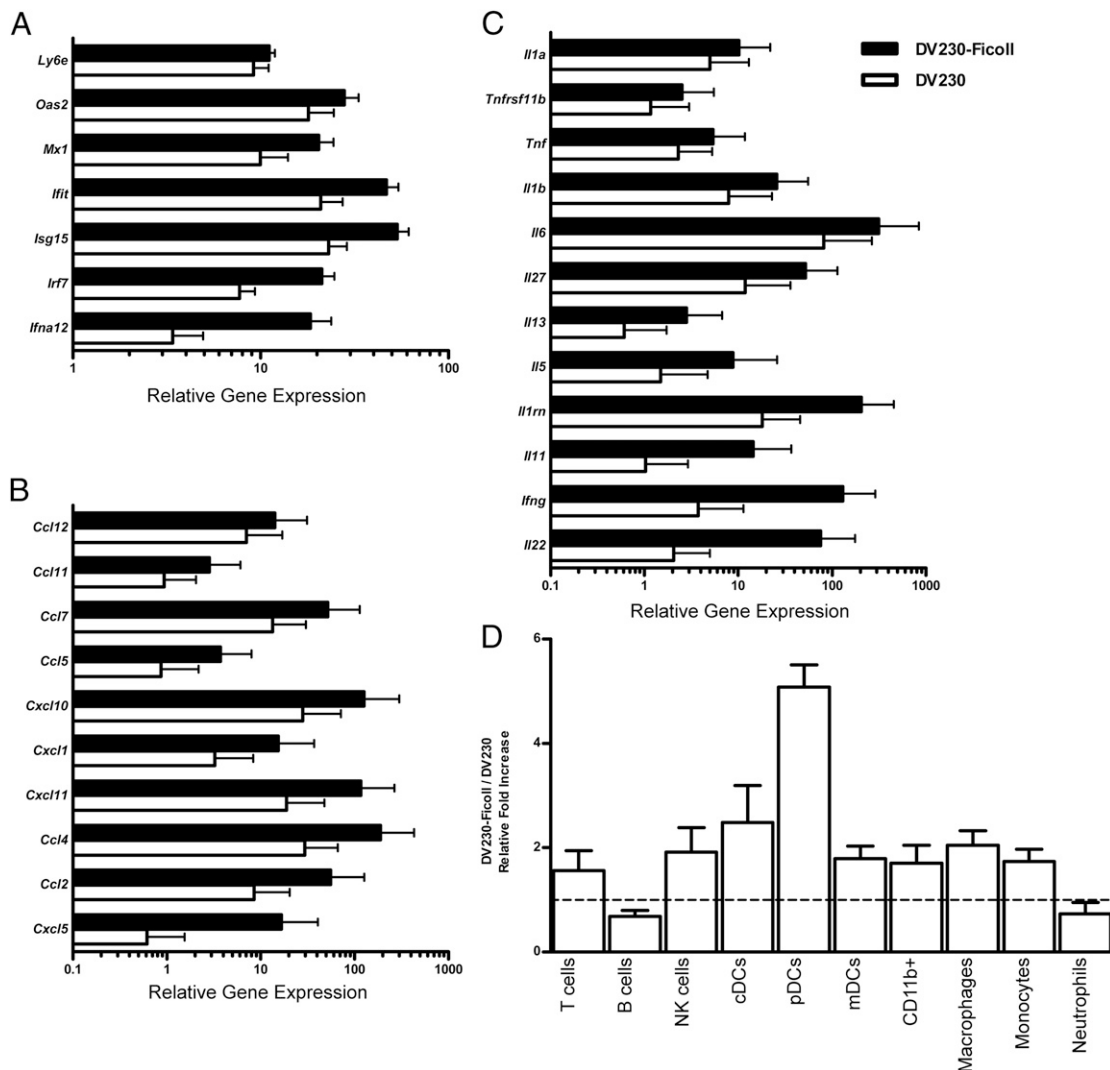
FIGURE 6. DV230-Ficoll nanoparticles enhance IFN-regulated, chemokine, and cytokine genes, leading to enhanced cell recruitment in draining lymph nodes. (**A–C**) BALB/c mice (*n* = 6) were immunized s.c. with 10 μg DV230-Ficoll or DV230. Popliteal lymph nodes were collected 6 h following immunization to assess (A) IFN-regulated, (B) chemokine, and (C) cytokine gene expression. Gene expression relative to PBS-injected controls was determined by ΔΔCt evaluation ($2^{-\Delta\Delta Ct}$). Data are shown as means of individual samples with 95% CI. Data are from a single experiment. (**D**) Relative proportions of different cell populations in popliteal lymph nodes of BALB/c mice (*n* = 4–6) immunized s.c. in footpads 48 h earlier with 10 μg DV230-Ficoll or DV230 in combination with 10 or 2 μg rPA were analyzed by flow cytometry. Following light scatter gating, cell populations were identified as follows: T cells (CD3$^+$/CD19$^-$), B cells (CD3$^-$/CD19$^+$), NK cells (CD3$^-$/CD19$^-$/CD49b$^+$), and the following CD3$^-$/CD19$^-$/CD49b$^-$ cell populations: cDCs (CD11b$^-$/CD11c$^+$/MHC II$^+$), pDCs (CD11b$^-$/CD11c$^+$/MHC II$^+$ /PDCA1$^+$ or B220$^+$), mDCs (CD11b$^+$/CD11c$^+$/MHC II$^+$), myeloid cells (CD11b$^+$/CD11c$^-$/MHC II$^+$), macrophages (CD11b$^+$/CD11c$^-$/MHC II$^+$/F4/80$^+$/Ly6C$^+$/Ly6G$^-$), monocytes (CD11b$^+$/CD11c$^-$/MHC II$^+$/F4/80$^-$/Ly6C$^+$/Ly6G$^-$), and neutrophils (CD11b$^+$/CD11c$^-$/Ly6G$^+$). Data are shown as means with SEM. Results are representative of four independent experiments.

cytometry. At 24 h, total CD45$^+$ cells were 3-fold as abundant in DV230-Ficoll–injected muscle compared with DV230-injected tissue (~212,000 versus ~67,000 cells/g muscle). DV230-Ficoll injection induced relatively higher proportions of conventional DCs (cDCs), myeloid DCs (mDCs), myeloid cells, macrophages, monocytes, and neutrophils in the injected muscle compared with mice administered monomeric DV230 (Fig. 4E).

To test whether DV230-Ficoll–induced inflammatory gene expression and adjuvanticity for rPA-induced Ab responses involved TLR9-independent pathways, responses were tested in TLR9$^{-/-}$ mice. Following i.m. injection with DV230-Ficoll, induction of IRGs and chemokine and cytokine genes was observed in wild-type C57BL/6 mice, but not in TLR9$^{-/-}$ mice (Fig. 5A). Consequently, no DV230-Ficoll adjuvant activity was observed in TLR9$^{-/-}$ mice (Fig. 5B). The lack of both inflammatory responses induced at the injection site and adjuvant effects in TLR9$^{-/-}$ mice demonstrates that the activity of DV230-Ficoll is entirely dependent on TLR9 signaling.

DV230-Ficoll nanoparticles augment lymph node gene expression and cellular infiltration

We next sought to investigate effects by monomeric and nanoparticle DV230 formulations within draining lymph nodes, where T and B cell responses are initiated (31). To more easily target and assess lymph node–specific responses, we injected formulations s.c. in the footpad. Prior to proceeding, we confirmed that the s.c. and i.m. routes induced equivalent TNA titers following rPA/DV230-Ficoll immunizations (Supplemental Fig. 2). Transcriptional changes induced within the draining lymph node by injection of DV230 or DV230-Ficoll was assessed by real-time PCR 18 h after s.c. injection. In lymph nodes, as in injection site muscle, DV230-Ficoll produced greater increases in transcription of IRGs (Fig. 6A), chemokines (Fig. 6B), and cytokines (Fig. 6C)

compared with DV230-Ficoll. As a likely consequence of stronger induction of multiple chemokines, DV230-Ficoll injection resulted in greater numbers of various APC populations in the draining lymph node compared with DV230-injected mice. MHC II$^+$ pDCs were especially affected, with 5-fold greater numbers present (mean, 940 versus 187 cells/lymph node) following DV230-Ficoll treatment (Fig. 6D). Taken together, these data suggest that DV230-Ficoll is more potent than monomeric DV230 for initiating immune responses at the injection site and in draining lymph nodes.

DV230-Ficoll nanoparticles are more efficient for uptake by and activation of APCs

Next, we addressed whether relative increases in cellular trafficking following DV230-Ficoll treatment were accompanied by differential effects on cellular uptake of the adjuvant. Comparison of DV230-Ficoll and DV230 labeled with Alexa Fluor 555 and administered at equivalent CpG-based doses showed DV230-Ficoll taken up to a greater extent than DV230 by lymph node cells. A wide range of cell populations involved in the initiation of adaptive immune response, including MHC II$^+$ pDCs and mDCs, myeloid cells, macrophages, and monocytes, as well as neutrophils, all demonstrated greater fluorescence following injection with DV230-Ficoll (Fig. 7A). There were substantial proportions of mDCs, myeloid cells, macrophages, and monocytes with high levels of Alexa Fluor 555 fluorescence in DV230-Ficoll–injected mice, whereas only mDCs internalized DV230 to a similar extent. Lymphocyte uptake of either Alexa Fluor 555–labeled DV230-Ficoll or DV230 was negligible (data not shown).

DV230-Ficoll also exerted a greater effect on the activation state of APCs and lymphocytes than did monomeric DV230 within the draining lymph nodes. Following DV230-Ficoll injection, pDCs, CD8$^+$ DCs, cDCs, mDCs, and myeloid cells all displayed greater
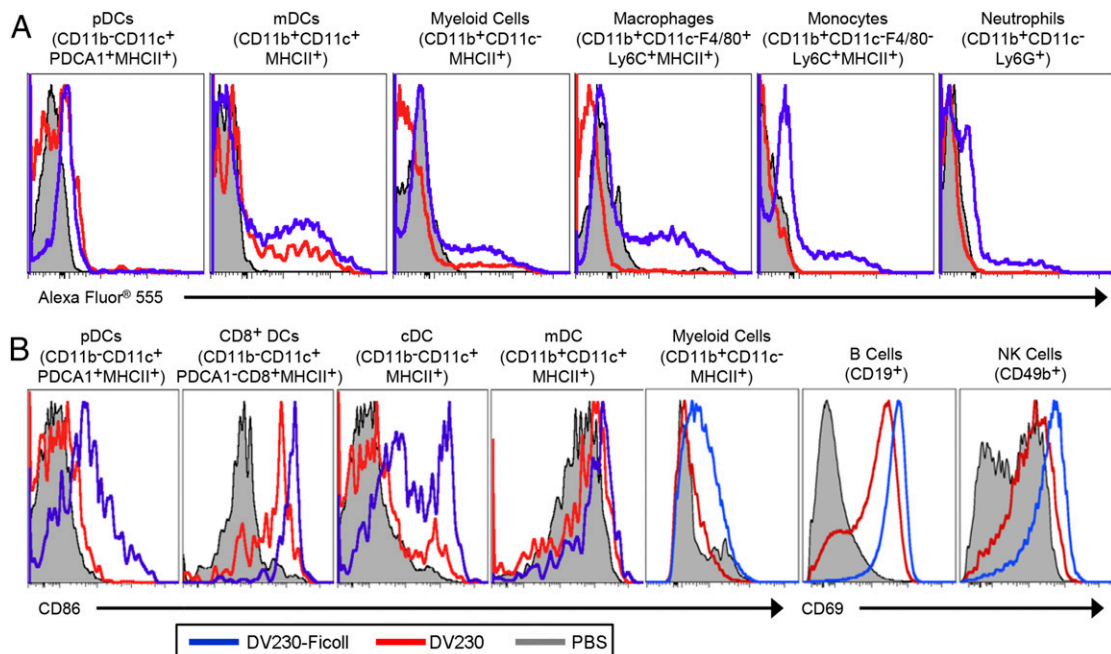
FIGURE 7. DV230-Ficoll nanoparticles are taken up by and induce maturation/activation of lymph node cells to a greater extent than monomeric DV230. (**A**) BALB/c mice ($n = 4$–6/group) were injected s.c. in footpads with 5 μg DV230-Ficoll–Alexa Fluor 555 or DV230–Alexa Fluor 555. Presence of labeled DV230-Ficoll or DV230 in pDCs, mDCs, myeloid cells, macrophages, monocytes, and neutrophils within pooled/group popliteal lymph nodes at 24 h was assessed by flow cytometry. Histogram data shown are representative of four independent experiments. (**B**) Expression of maturation marker CD86 on pDCs, CD8$^+$ DCs (CD3$^-$/CD19$^-$/CD49b$^-$/CD11c$^+$/PDCA1$^-$ or B220$^-$/CD8$^+$), cDCs, mDCs, or myeloid cells and CD69 expression on B cells and NK cells in pooled popliteal lymph nodes at 20 h after s.c. footpad injection with 5 μg DV230-Ficoll or DV230 were assessed by flow cytometry. Histogram data shown are representative of three independent experiments.

expression of CD86, whereas B and NK cells displayed greater expression of CD69 (Fig. 7B) compared with lymph node cells harvested from mice injected with monomeric DV230. Thus, nanoparticulate formulation of DV230 on Ficoll substantially improves its uptake by and activation of key APC populations, contributing to the effective induction of adaptive immunity.

DV230-Ficoll nanoparticles enhance joint uptake of coinjected Ag and adjuvant in APCs and augment the nascent adaptive immune response

There is considerable evidence that TLR enhancement of adaptive immunity is most efficient when it acts on APCs that have acquired and processed the relevant Ag (32, 33). To determine whether Ficoll conjugation increases the efficiency of CpG-ODN and Ag uptake into the same cells, mice received footpad injections with fluorescently labeled adjuvants (as described above) plus rPA labeled with Alexa Fluor 647. Popliteal lymph node cells were harvested 24 or 48 h after injection for flow cytometry analysis. For each APC type examined, many cells incorporated only Ag or adjuvant; however, there was also a population of cells that acquired both rPA and DV230-Ficoll or DV230. Mice immunized with DV230-Ficoll and rPA demonstrated the highest frequency of APCs with coincident Ag and adjuvant uptake as well as cells with adjuvant uptake only (Fig. 8A; 48 h data shown).

As colocalization of Ag and adjuvant within the same endosomal compartment has been associated with optimal MHC II Ag presentation (34), we employed polychromatic imaging flow cytometry and subsequent calculation of BDS scoring in two additional experiments to determine whether Alexa Fluor 555–labeled DV230-Ficoll and Alexa Fluor 647–labeled rPA specifically colocalized within the same cells. Approximately 11% of pDCs, 7% of mDCs, 5% of myeloid cells, and <1% of cDCs with joint DV230-Ficoll and rPA uptake demonstrated BDS scores > 2, indicating likely colocalization of Ag and adjuvant within cells at the time of measurement. Examples of pDC, cDC, mDC, and myeloid cells showing Ag and adjuvant colocalization are shown in Fig. 8B.

One likely mechanism for the increased speed and efficacy of DV230-Ficoll as an adjuvant is an enhancement of GC B and T follicular helper (T$_{FH}$) cell responses within the injection site draining lymph nodes. This was directly evaluated by flow cytometry, identifying GC B cells as CD45R$^+$/GL7$^+$/PNA$^+$/CD95$^+$ cells and T$_{FH}$ cells as CD4$^+$/CXCR5$^+$/CD279$^+$ cells (Fig. 9A). Mice were immunized once in the footpad with rPA with/without DV230-Ficoll or DV230 or vehicle control, with numbers of GC B or T$_{FH}$ cells monitored for 2 wk. Higher proportions of GC B and T$_{FH}$ cells were detected in draining lymph nodes of rPA/DV230-Ficoll immunized mice by day 5 and remained elevated at 14 d
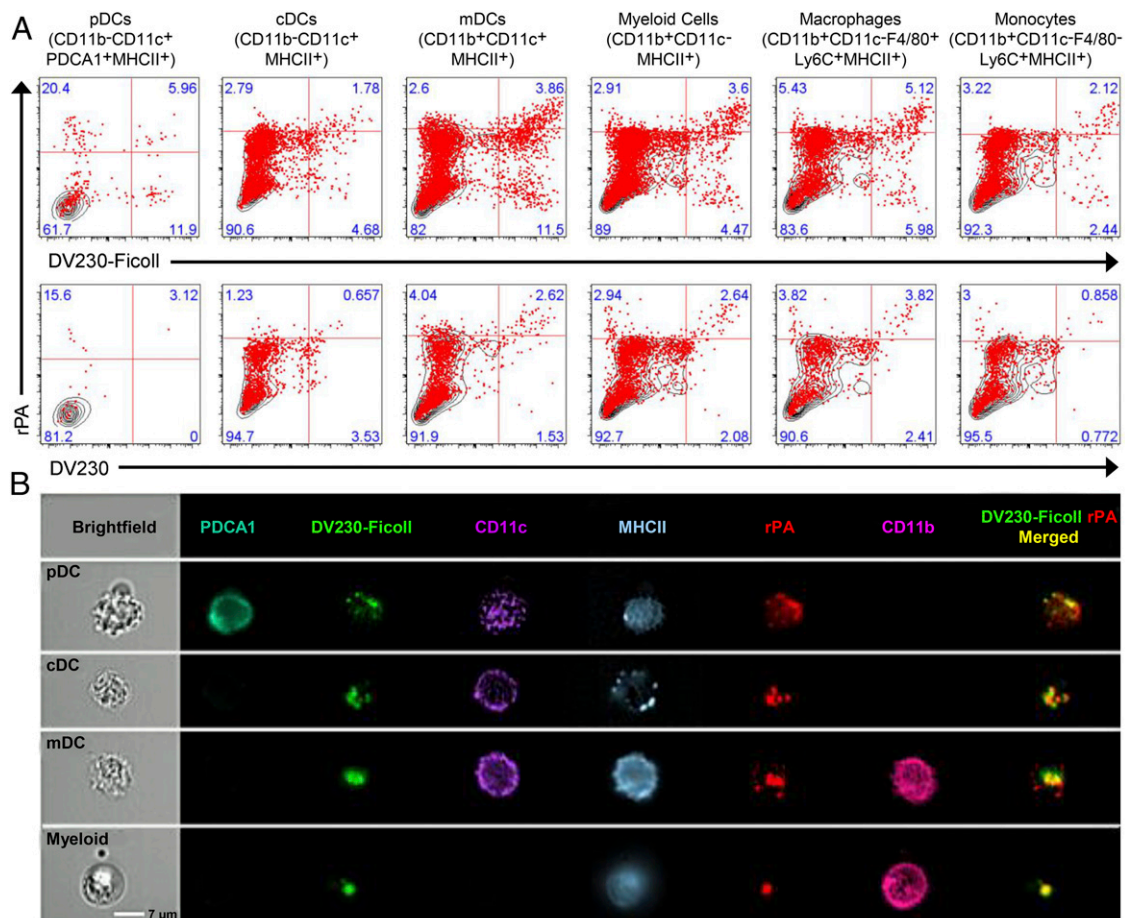
FIGURE 8. DV230-Ficoll nanoparticles promote joint uptake of Ag and adjuvant in immunized mice. BALB/c mice (*n* = 4/group) were immunized s.c. in footpads with 10 μg Alexa Fluor 647–labeled rPA in combination with 10 μg Alexa Fluor 555–labeled DV230-Ficoll or DV230. (**A**) Presence of labeled rPA and DV230-Ficoll in MHC II$^+$ pDC, cDC, mDC, myeloid cells, macrophages, and monocytes at 48 h in the popliteal lymph nodes (pooled/group) was assessed by flow cytometry. Black contour lines indicate DPBS control. Data shown are representative of two independent experiments. (**B**) ImageStream analysis was performed to detect labeled rPA and DV230-Ficoll in MHC II$^+$ pDCs, cDCs, mDCs, and myeloid cells harvested from popliteal lymph nodes at 24 h. Colocalization of fluorescent Ag and adjuvant within specific cells is shown in merged images at the end of each row. Data are representative of two independent experiments. Scale bar, 7μm.

(Fig. 9B, 9C). GC B and T$_{FH}$ responses were minimal in rPA only immunized mice compared with vehicle-injected mice. Taken together, these data suggest that the increased potency of DV230-Ficoll over DV230 for induction of innate immunity is reflected in early GC B and T cell responses.

DV230-Ficoll nanoparticles demonstrate preferential local retention with reduced systemic distribution

Increased potency for induction of innate immune responses and subsequent development of high-titer Ab responses may reflect, in part, increased local retention of active CpG-ODN at the injection site and draining lymph nodes. To test whether DV230-Ficoll and monomeric DV230 display differential tissue distribution kinetics following i.m. injection, we injected mice with DV230-Ficoll or DV230 and measured levels of the adjuvants at the injection site and draining lymph nodes as well as at distal sites (spleen, liver, and kidney). Mice received a high dose (100 μg) of either adjuvant to facilitate recovery, and tissues were harvested 1 d after injection. DV230-Ficoll and DV230 were quantified by hybridization assays. DV230-Ficoll was concentrated in injection site muscle and lymph nodes (popliteal, inguinal, sciatic, lumbar, and sacral), whereas DV230 quickly distributed systemically (Fig. 10). DV230 was detected at minimal levels at the injection site and lymph nodes, and instead concentrated in the spleen, liver, and kidney. These data indicate that nanoparticle and monomeric DV230 differentially distribute within 24 h of injection, suggesting that preferential local retention of DV230-Ficoll may contribute to its increased potency as an adjuvant.

DV230-Ficoll nanoparticles exhibit reduced systemic toxicity

The ability of DV230-Ficoll to concentrate largely in the injected muscle and lymph nodes, rather than to distribute systemically, suggested that an altered profile of systemic toxicities might be observed with high, repetitive dosing. To test this, mice were given four biweekly i.m. injections with a high dose (100 μg) of DV230-Ficoll or DV230. All of the systemic toxicities commonly observed in mice following CpG-ODN administration were greatly reduced in animals injected with DV230-Ficoll compared with DV230. Specifically, whereas DV230 induced high levels of serum cytokines IL-6, IL-12p40, and TNF-α at 2 h postinjection, these inflammatory cytokines were not induced at appreciable levels in DV230-Ficoll–injected mice (Fig. 11A). Additionally, there was little evidence of a delayed systemic effect in DV230-

Ficoll–injected mice. Mice sacrificed after four biweekly injections of DV230-Ficoll demonstrated spleen and liver weights similar to sham-injected mice, whereas splenomegaly and hepatomegaly were evident in mice given four biweekly DV230 injections (Fig. 11B). Histopathological changes in DV230-Ficoll–injected mice were minimal, whereas repeated DV230 injections resulted in increased splenic extramedullary hematopoietic activity and hepatic changes, including cellular infiltration of sinusoids, hepatocellular alterations, and mild/moderate liver necrosis (data not shown), all of which are known class effects of phosphorothioate oligonucleotides in mice (35, 36). Lastly, marked body weight loss, a TNF-α–dependent, CpG-induced toxicological event specific to rodents (37), occurred in animals administered biweekly DV230 injections (Fig. 11C; data shown are adjusted for effects of splenomegaly and hepatomegaly). In contrast, body weights were only slightly lower than those of controls for mice administered biweekly injections of high-dose DV230-Ficoll. Thus, the improved adjuvant activity of DV230-Ficoll nanoparticles over monomeric DV230 is accompanied by reduced systemic toxicity signals.

Discussion

In this study, we show that the magnitude and kinetics of the neutralizing Ab response to *B. anthracis* rPA in primates are greatly enhanced by covalent linkage of the CpG-ODN DV230 to the high molecular mass sucrose polymer Ficoll. The resulting DV230-Ficoll nanoparticles were especially potent at enhancing the primary immune response to rPA, with rapid induction of protective TNA responses and complete protection of cynomolgus monkeys against a high-dose aerosolized anthrax challenge after a single immunization. Comparisons between DV230 and DV230-Ficoll in mice demonstrated that the greater efficacy of DV230-Ficoll resulted from greater activity at multiple steps in the innate and early adaptive immune response. DV230-Ficoll was largely retained at the injection site and draining lymph nodes, increasing its local concentration, stimulating enhanced Ag uptake by and activation of APCs, and augmenting infiltration of multiple immune cell types into the node. In contrast, monomeric DV230 quickly distributed systemically after injection, reducing its efficacy at the sites relevant for generating an immune response, and, at high doses, generating inflammatory responses responsible for the systemic toxicities typical of high doses of CpG-ODNs in
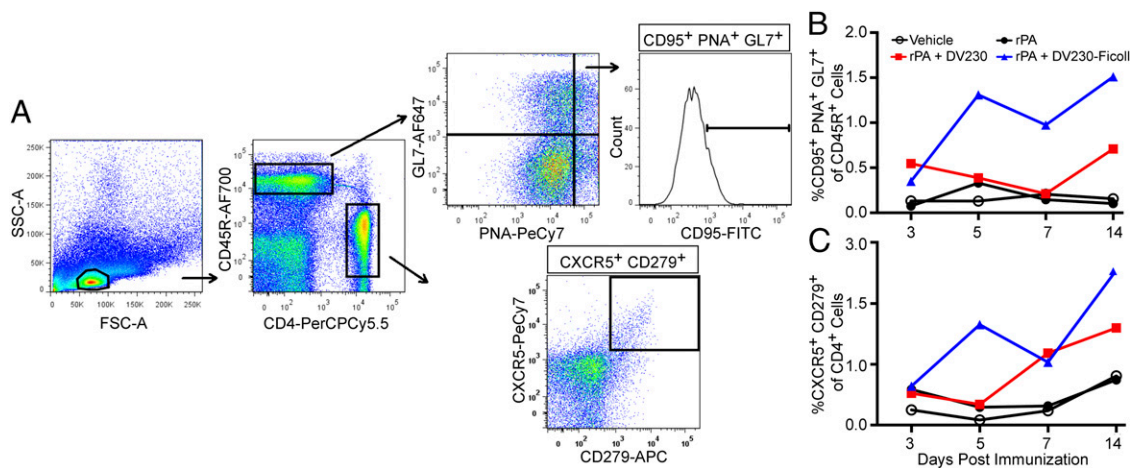
FIGURE 9. rPA/DV230-Ficoll immunization promotes lymph node GC B cell and T$_{FH}$ cell expansion. BALB/c mice (*n* = 5/group) were immunized s.c. in footpads with 2 μg rPA in combination with 2 μg DV230-Ficoll or DV230. (**A**) Gating strategies for CD45R$^+$/CD4$^-$/CD95$^+$/PNA$^+$/GL7$^+$ GC B cells and CD4$^+$/CD45R$^-$/CXCR5$^+$/CD279$^+$ T$_{FH}$ cells in total lymph node cell populations are shown. Percentages of (**B**) GC B or (**C**) T$_{FH}$ cells were monitored for 14 d following immunization. Data shown are representative of three independent experiments.

FIGURE 10. DV230-Ficoll nanoparticles are preferentially retained at the injection site and draining lymph nodes. BALB/c mice (*n* = 5) were injected i.m. with 100 μg DV230-Ficoll or DV230. Oligonucleotide content (micrograms per gram of tissue) in injection site muscle, draining lymph nodes (popliteal, inguinal, sciatic, lumbar, and sacral), spleen, liver, and kidney was assessed at 1 d postinjection. Data are shown with means. Data are representative of two independent experiments.
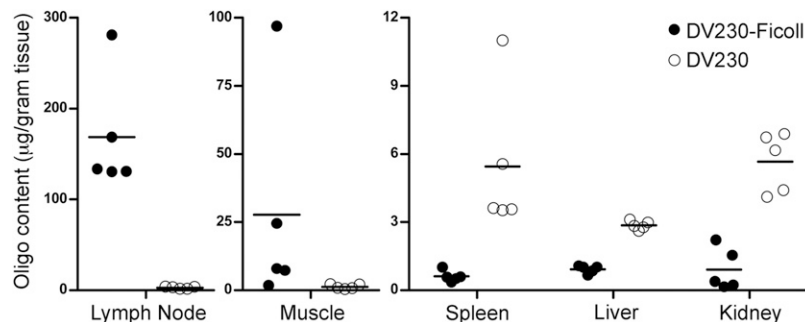
mice. Thus, although CpG-ODN adjuvants have demonstrated improvement over alum for induction of high-titer Ab responses in humans with fewer immunizations (4), multimeric presentation of CpG-ODN on a Ficoll scaffold further augments adjuvant activity, potentially enabling single immunization protection to a variety of emerging infectious diseases or bioterror agents.

We chose anthrax rPA as the Ag with which to test DV230-Ficoll as an improved adjuvant for generating rapid and potent immunogenicity in primates. The potential use of anthrax as a bioterror agent and the multiple-immunization regimen recommended for the current U.S.-licensed vaccine, AVA, demonstrate a need for a rapid-acting vaccine with a reduced, preferably single, injection regimen (17). Additionally, as a single, well-defined, recombinant protein, rPA represents an attractive Ag alternative to that found in AVA, which although containing predominantly PA absorbed to alum, also contains other Ags and is of undefined composition with lot-to-lot variation (38). A number of studies in monkeys, a suitable surrogate for predicting the human anthrax vaccine response (39), have shown complete protection against lethal aerosolized anthrax challenge following a two- to three-immunization regimen of AVA or rPA on alum (39–42), but complete protection following a single immunization has yet to be demonstrated in these animals. Thus, the ability of CpG-ODN to promote rapid, high-titer, and durable Ab responses to Ags makes this class of adjuvant a strong candidate for improving the rapidity and magnitude of Ab responses to vaccines against potential biological warfare agents such as anthrax. The addition of CpG 7909 (a B class CpG-ODN) to AVA accelerated the induction of post–secondary Ab responses and TNA titers in clinical trials with two- or three-immunization regimens (43, 44) and, as a two-immunization regimen, had similar effects in monkeys, although protection was not evaluated (45). However, responses following primary immunization with AVA were minimal in the clinical studies and were not enhanced by addition of CpG to the alum-adjuvanted vaccine. We focused on alternative formulation of the CpG DV230, rather than a CpG/alum adjuvant combination approach, to improve the primary response to anthrax rPA. The present study, in which monkeys were immunized with rPA and DV230-Ficoll, is, to our knowledge, the first published report to demonstrate 100% protection of NHPs against aerosolized anthrax challenge following a single immunization. This protection was associated with high TNA titers (mean > 1000 and significantly higher than rPA alone) as early as 2 wk after primary immunization as well as a rapid rise in titers in the days immediately following aerosol challenge. After infection, animals immunized only once quickly generated TNA titers comparable to those of monkeys immunized twice, demonstrating the induction of effective immunological memory following a single rPA/DV230-Ficoll immunization.

A variety of adjuvants, including a number of nanoparticle-like formulations, have been tested in preclinical anthrax prophylaxis

vaccine models. Among such approaches, monophosphoryl lipid A–containing liposomes mixed with or containing rPA proved successful at inducing high-titer TNA responses in monkeys after two immunizations and complete protection from aerosolized spore challenge after three immunizations (46). For CpG-ODN, additional delivery options include liposomal encapsulation or packaging as polylactide–co-glycide microparticles (47, 48). Improved anti-PA Ab titers and partial protection against i.p. anthrax spore challenge were demonstrated in mice immunized once with CpG-ODN absorbed onto polylactide–co-glycide microparticles and mixed with AVA (49). PA expressed in an adenovirus vector has been tested in rodents with 100% protection against anthrax challenge after a single intranasal or i.m. immunization in mice or rats, respectively (50, 51). However, pre-existing intranasally induced immunity to Ad5 did inhibit subsequent i.m. immunization-induced Ab responses in the rats. Additional adjuvant approaches that have demonstrated protective efficacy in mice with two injection regimens include immunization with rPA and combined Advax and murabutide adjuvants or immunization with acetalated dextran microparticles encapsulating rPA and the TLR7/8 agonist resiquimod (52, 53). In comparison with these approaches, the DV230-Ficoll adjuvant offers a number of advantages in the context of anthrax vaccine development, and possibly as an adjuvant for other Ags for which especially rapid responses are required. In addition to inducing high-titer functional Ab responses that are protective after a single immunization in primates, admixture of Ag and DV230-Ficoll represents a simple, flexible approach. The Ficoll platform itself is considered nonimmunogenic (54), and chemistry for covalent linkage of molecules such as DV230 to Ficoll has been well characterized (20). DV230-Ficoll, unlike alum, offers the flexibility of a lyophilized vaccine composition, eliminating dependence on the cold-chain for long-term preservation.

DV230-Ficoll's basic physicochemical attributes of size (~50 nm) and multimeric CpG presentation (~120 CpG-ODN/Ficoll particle) mimic key features of virus-like particles that are known to improve immunogenicity (8). Hence, we investigated whether the improved ability of DV230-Ficoll over DV230 for generating rapid, high-titer rPA-specific Ab responses was associated with relative differences in induction of innate immune responses at the injection site and draining lymph nodes. At both sites, DV230 and DV230-Ficoll induced the expression of a range of genes comparable to what has been previously reported at the injection site in mice in response to other CpG-ODNs (55, 56). However, DV230-Ficoll consistently induced greater expression of each individual gene when compared with an equivalent dose of DV230. This quantitative difference in inflammatory and chemokine-associated gene induction was reflected in relative increases in various CD45^{+} cell populations at the injection site and draining lymph nodes of DV230-Ficoll–injected mice. In addition to these effects, adjuvants may enhance immune responses
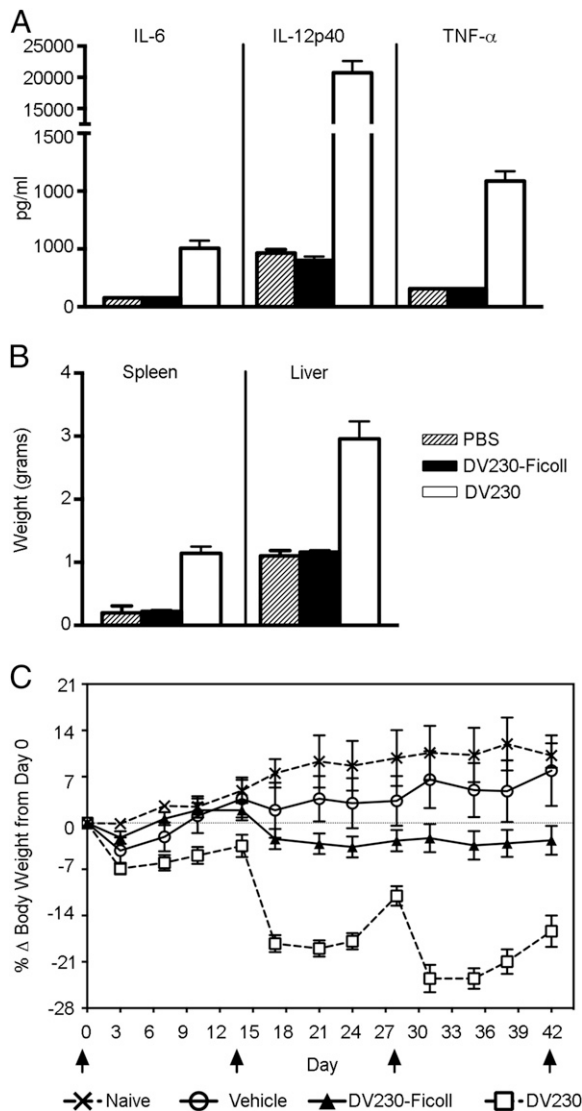
FIGURE 11. Systemic toxicity signals are greatly reduced in response to DV230-Ficoll nanoparticles as compared with nonconjugated DV230. BALB/c mice ($n = 5$) were injected with 100 μg DV230-Ficoll or DV230 on days 0, 14, 28, and 42. (**A**) Serum cytokine levels measured 2 h following first injection and (**B**) organ weights measured 18 h following day 42 injection are shown. (**C**) Mean body weights per treatment condition are shown. Injection time points are indicated by arrowheads. To adjust for effect of hepatomegaly and splenomegaly on body weight, liver and spleen weights at sacrifice on day 14, 28, or 42 were subtracted from body weights recorded on days 14, 17, 21, and 24, on days 28, 31, 35 and 38, or on day 42, respectively. All data are shown as means with SEM. Data shown are representative of two independent experiments.

by activating maturation of and increasing Ag uptake by APCs (57). Within the draining lymph nodes, the adjuvant DV230-Ficoll (compared with DV230) was taken up to a greater extent by, and induced greater maturation in, pDCs and other APC populations, as measured by CD86 expression. In contrast, although adjuvant uptake by lymphocytes was low (data not shown), DV230-Ficoll–injected mice nonetheless demonstrated higher CD69 expression on B cells and NK cells. Taken together, our findings demonstrate that formulating DV230 on Ficoll results in much more effective innate immune induction, including activation/maturation of key APC populations. The potential importance of these early responses to the rapid induction of high-titer Ab following rPA/DV230-Ficoll immunization is suggested by indirect comparison with anthrax

vaccine, precipitated (the licensed U.K. vaccine), which has been reported to be a poor inducer of DC maturation, perhaps partly explaining the need for repeated immunizations (58).

Studies tracking uptake of both fluorescently labeled Ag and adjuvant further demonstrated that DV230-Ficoll, compared with DV230, also promoted increased co-uptake of both rPA and adjuvant into the same cells. This represents a potential mechanistic advantage for DV230-Ficoll over DV230, as coantigen and adjuvant delivery to a DC is critical to efficiently prime immune responses as opposed to induce tolerance (59, 60). In separate experiments using polychromatic imaging flow cytometry and focusing only on rPA/DV230-Ficoll immunized mice, we found that a proportion of cells specifically demonstrated intracellular colocalization of rPA and DV230-Ficoll, which is associated with optimal MHC II Ag presentation (34). This augmented APC uptake of both Ag and adjuvant in rPA/DV230-Ficoll immunized mice was further associated with a relative increase in early lymph node GC B cell and T_{FH} responses, which may also be a contributory mechanism explaining the relatively increased adjuvant activity of DV230-Ficoll on anti-rPA Ab titers. For example, it has recently been shown that human blood T_{FH} responses emerging by day 7 postvaccination with nonadjuvanted trivalent split influenza vaccine correlated with increases in pre-existing Ab responses (61). In that study, the T_{FH} cells provided help to memory, but not naive, B cells, prompting the authors to speculate that, as demonstrated in mice, addition of a TLR-stimulating adjuvant to the split vaccine may be required to initiate primary responses (62).

In addition to the increased efficacy of DV230-Ficoll, the preferential retention of a TLR9 ligand at the injection site and draining lymph node reduced systemic exposure and substantially attenuated the systemic toxicities typical of high-dose exposure to TLR9 agonists in mice. DV230-Ficoll was predominantly localized to the injection site muscle and draining lymph nodes after injection, whereas DV230 was concentrated in distal organs, principally spleen, liver, and kidney. Thus, local retention of DV230-Ficoll corresponded to both increased adjuvant activity and substantially reduced acute (i.e., elevated serum cytokine levels at 2 h postinjection) and chronic (i.e., splenomegaly, hepatomegaly, and body weight loss) toxicities after a series of four biweekly injections. These DV230-Ficoll findings are in agreement with data on other CpG-ODN adjuvant nanoparticle formulations or lymph node–targeting approaches that resulted in increased potency and decreased systemic toxicity signals (63, 64).

In summary, covalent attachment of DV230 (a CPG-ODN molecule) to the sucrose polymer Ficoll markedly augments adjuvant activity as demonstrated in both NHPs and mice. DV230-Ficoll, but not DV230, when mixed with rPA from *B. anthracis*, significantly enhances immunogenicity compared with rPA immunization alone, resulting in high titers of neutralizing Abs as early as 2 wk after immunization. TNA titers elicited by a single immunization of rPA/DV230-Ficoll completely protected monkeys from lethal aerosol spore challenge. At multiple steps in the induction of immunity, DV230-Ficoll demonstrated stronger adjuvant activity compared with DV230. DV230-Ficoll elicited stronger IFN and inflammatory gene expression as well as greater cellular influx at the injection site and draining lymph nodes. DV230-Ficoll facilitated enhanced uptake by key APC populations, resulting in greater induction of maturation marker expression, and promoted joint uptake of Ag, generating more rapid and stronger GC B and T cell responses. In terms of mechanism of action, the relative advantage of DV230-Ficoll over DV230 may be mediated, at least in part, by improved retention at the injection site and draining lymph nodes. Taken together, these data demonstrate that rPA/DV230-Ficoll represents an attractive, practical

option for generation of rapid, potent single-immunization–induced humoral immune responses against anthrax. Additionally, given the rapidity of response to a single immunization, DV230-Ficoll may also represent an attractive adjuvant for use in postexposure prophylaxis regimens.

Acknowledgments

Disclosures

References

1. Krieg, A. M. 2006. Therapeutic potential of Toll-like receptor 9 activation. *Nat. Rev. Drug Discov.* 5: 471–484.
2. Bode, C., G. Zhao, F. Steinhagen, T. Kinjo, and D. M. Klinman. 2011. CpG DNA as a vaccine adjuvant. *Expert Rev. Vaccines* 10: 499–511.
3. Eng, N. F., N. Bhardwaj, R. Mulligan, and F. Diaz-Mitoma. 2013. The potential of 1018 ISS adjuvant in hepatitis B vaccines: HEPLISAV™ review. *Hum. Vaccin. Immunother.* 9: 1661–1672.
4. Halperin, S. A., B. Ward, C. Cooper, G. Predy, F. Diaz-Mitoma, M. Dionne, J. Embree, A. McGeer, P. Zickler, K. H. Moltz, et al. 2012. Comparison of safety and immunogenicity of two doses of investigational hepatitis B virus surface antigen co-administered with an immunostimulatory phosphorothioate oligodeoxyribonucleotide and three doses of a licensed hepatitis B vaccine in healthy adults 18–55 years of age. *Vaccine* 30: 2556–2563.
5. Sablan, B. P., D. J. Kim, N. G. Barzaga, W. C. Chow, M. Cho, S. H. Ahn, S. G. Hwang, J. H. Lee, H. Namini, and W. L. Heyward. 2012. Demonstration of safety and enhanced seroprotection against hepatitis B with investigational HBsAg-1018 ISS vaccine compared to a licensed hepatitis B vaccine. *Vaccine* 30: 2689–2696.
6. Janssen, J. M., W. L. Heyward, J. T. Martin, and R. S. Janssen. 2015. Immunogenicity and safety of an investigational hepatitis B vaccine with a Toll-like receptor 9 agonist adjuvant (HBsAg-1018) compared with a licensed hepatitis B vaccine in patients with chronic kidney disease and type 2 diabetes mellitus. *Vaccine* 33: 833–837.
7. Oyewumi, M. O., A. Kumar, and Z. Cui. 2010. Nano-microparticles as immune adjuvants: correlating particle sizes and the resultant immune responses. *Expert Rev. Vaccines* 9: 1095–1107.
8. Bachmann, M. F., and G. T. Jennings. 2010. Vaccine delivery: a matter of size, geometry, kinetics and molecular patterns. *Nat. Rev. Immunol.* 10: 787–796.
9. Kasturi, S. P., I. Skountzou, R. A. Albrecht, D. Koutsonanos, T. Hua, H. I. Nakaya, R. Ravindran, S. Stewart, M. Alam, M. Kwissa, et al. 2011. Programming the magnitude and persistence of antibody responses with innate immunity. *Nature* 470: 543–547.
10. Marshall, J. D., D. Higgins, C. Abbate, P. Yee, G. Teshima, G. Ott, T. dela Cruz, D. Passmore, K. L. Fearon, S. Tuck, and G. Van Nest. 2004. Polymyxin B enhances ISS-mediated immune responses across multiple species. *Cell. Immunol.* 229: 93–105.
11. Wilson, J. T., S. Keller, M. J. Manganiello, C. Cheng, C. C. Lee, C. Opara, A. Convertine, and P. S. Stayton. 2013. pH-responsive nanoparticle vaccines for dual-delivery of antigens and immunostimulatory oligonucleotides. *ACS Nano* 7: 3912–3925.
12. Kobiyama, K., T. Aoshi, H. Narita, E. Kuroda, M. Hayashi, K. Tetsutani, S. Koyama, S. Mochizuki, K. Sakurai, Y. Katakai, et al. 2014. Nonagonistic Dectin-1 ligand transforms CpG into a multitask nanoparticulate TLR9 agonist. *Proc. Natl. Acad. Sci. USA* 111: 3086–3091.
13. Marshall, J. D., E. M. Hessel, J. Gregorio, C. Abbate, P. Yee, M. Chu, G. Van Nest, R. L. Coffman, and K. L. Fearon. 2003. Novel chimeric immunomodulatory compounds containing short CpG oligodeoxyribonucleotides have differential activities in human cells. *Nucleic Acids Res.* 31: 5122–5133.
14. Guiducci, C., G. Ott, J. H. Chan, E. Damon, C. Calacsan, T. Matray, K. D. Lee, R. L. Coffman, and F. J. Barrat. 2006. Properties regulating the nature of the plasmacytoid dendritic cell response to Toll-like receptor 9 activation. *J. Exp. Med.* 203: 1999–2008.
15. Amlot, P. L., A. E. Hayes, D. Gray, E. C. Gordon-Smith, and J. H. Humphrey. 1986. Human immune responses in vivo to protein (KLH) and polysaccharide (DNP-Ficoll) neoantigens: normal subjects compared with bone marrow transplant patients on cyclosporine. *Clin. Exp. Immunol.* 64: 125–135.
16. Schwander, S., M. Opravil, R. Lüthy, D. G. Hanson, J. Schindler, A. Dawson, B. Letwin, and M. Dietrich. 1994. Phase I/II vaccination study of recombinant peptide F46 corresponding to the HIV-1 transmembrane protein coupled with 2.4 dinitrophenyl (DNP) Ficoll. *Infection* 22: 86–91.
17. Wright, J. G., C. P. Quinn, S. Shadomy, and N. Messonnier, Centers for Disease Control and Prevention (CDC). 2010. Use of anthrax vaccine in the United States: recommendations of the Advisory Committee on Immunization Practices (ACIP), 2009. *MMWR Recomm. Rep.* 59(RR-6): 1–30.
18. Plotkin, S. A. 2010. Correlates of protection induced by vaccination. *Clin. Vaccine Immunol.* 17: 1055–1065.
19. Fay, M. P., D. A. Follmann, F. Lynn, J. M. Schiffer, G. V. Stark, R. Kohberger, C. P. Quinn, and E. O. Nuzum. 2012. Anthrax vaccine-induced antibodies provide cross-species prediction of survival to aerosol challenge. *Sci. Transl. Med.* 4: 151ra126.
20. Inman, J. K. 1975. Thymus-independent antigens: the preparation of covalent, hapten-Ficoll conjugates. *J. Immunol.* 114: 704–709.
21. Hemmi, H., O. Takeuchi, T. Kawai, T. Kaisho, S. Sato, H. Sanjo, M. Matsumoto, K. Hoshino, H. Wagner, K. Takeda, and S. Akira. 2000. A Toll-like receptor recognizes bacterial DNA. *Nature* 408: 740–745.
22. Hering, D., W. Thompson, J. Hewetson, S. Little, S. Norris, and J. Pace-Templeton. 2004. Validation of the anthrax lethal toxin neutralization assay. *Biologicals* 32: 17–27.
23. Hessel, E. M., M. Chu, J. O. Lizcano, B. Chang, N. Herman, S. A. Kell, M. Wills-Karp, and R. L. Coffman. 2005. Immunostimulatory oligonucleotides block allergic airway inflammation by inhibiting Th2 cell activation and IgE-mediated cytokine induction. *J. Exp. Med.* 202: 1563–1573.
24. Beum, P. V., M. A. Lindorfer, B. E. Hall, T. C. George, K. Frost, P. J. Morrissey, and R. P. Taylor. 2006. Quantitative analysis of protein co-localization on B cells opsonized with rituximab and complement using the ImageStream multispectral imaging flow cytometer. *J. Immunol. Methods* 317: 90–99.
25. Verthelyi, D., R. T. Kenney, R. A. Seder, A. A. Gam, B. Friedag, and D. M. Klinman. 2002. CpG oligodeoxynucleotides as vaccine adjuvants in primates. *J. Immunol.* 168: 1659–1663.
26. Ketloy, C., A. Engering, U. Srichairatanakul, A. Limsalakpetch, K. Yongvanitchit, S. Pichyangkul, and K. Ruxrungtham. 2008. Expression and function of Toll-like receptors on dendritic cells and other antigen presenting cells from non-human primates. *Vet. Immunol. Immunopathol.* 125: 18–30.
27. Vasconcelos, D., R. Barnewall, M. Babin, R. Hunt, J. Estep, C. Nielsen, R. Carnes, and J. Carney. 2003. Pathology of inhalation anthrax in cynomolgus monkeys (*Macaca fascicularis*). *Lab. Invest.* 83: 1201–1209.
28. Henning, L. N., J. E. Comer, G. V. Stark, B. D. Ray, K. P. Tordoff, K. A. Knostman, and G. T. Meister. 2012. Development of an inhalational *Bacillus anthracis* exposure therapeutic model in cynomolgus macaques. *Clin. Vaccine Immunol.* 19: 1765–1775.
29. Krieg, A. M. 2002. CpG motifs in bacterial DNA and their immune effects. *Annu. Rev. Immunol.* 20: 709–760.
30. Kawai, T., and S. Akira. 2010. The role of pattern-recognition receptors in innate immunity: update on Toll-like receptors. *Nat. Immunol.* 11: 373–384.
31. Manolova, V., A. Flace, M. Bauer, K. Schwarz, P. Saudan, and M. F. Bachmann. 2008. Nanoparticles target distinct dendritic cell populations according to their size. *Eur. J. Immunol.* 38: 1404–1413.
32. Maurer, T., A. Heit, H. Hochrein, F. Ampenberger, M. O'Keeffe, S. Bauer, G. B. Lipford, R. M. Vabulas, and H. Wagner. 2002. CpG-DNA aided cross-presentation of soluble antigens by dendritic cells. *Eur. J. Immunol.* 32: 2356–2364.
33. Kool, M., C. Geurtsvankessel, F. Muskens, F. B. Madeira, M. van Nimwegen, H. Kuipers, K. Thielemans, H. C. Hoogsteden, H. Hammad, and B. N. Lambrecht. 2011. Facilitated antigen uptake and timed exposure to TLR ligands dictate the antigen-presenting potential of plasmacytoid DCs. *J. Leukoc. Biol.* 90: 1177–1190.
34. Blander, J. M., and R. Medzhitov. 2006. Toll-dependent selection of microbial antigens for presentation by dendritic cells. *Nature* 440: 808–812.
35. Monteith, D. K., S. P. Henry, R. B. Howard, S. Flournoy, A. A. Levin, C. F. Bennett, and S. T. Crooke. 1997. Immune stimulation—a class effect of phosphorothioate oligodeoxynucleotides in rodents. *Anticancer Drug Des.* 12: 421–432.
36. Levin, A. A., S. P. Henry, D. Monteith, and M. V. Templin. 2001. Toxicity of antisense oligonucleotides. In *Antisense Drug Technology: Principles, Strategies and Applications.* S. T. Crooke, ed. Dekker, New York, p. 201–267.
37. Campbell, J. D., Y. Cho, M. L. Foster, H. Kanzler, M. A. Kachura, J. A. Lum, M. J. Ratcliffe, A. Sathe, A. J. Leishman, A. Bahl, et al. 2009. CpG-containing immunostimulatory DNA sequences elicit TNF-α–dependent toxicity in rodents but not in humans. *J. Clin. Invest.* 119: 2564–2576.
38. Friedlander, A. M., and S. F. Little. 2009. Advances in the development of next-generation anthrax vaccines. *Vaccine* 27(Suppl 4): D28–D32.
39. Quinn, C. P., C. L. Sabourin, N. A. Niemuth, H. Li, V. A. Semenova, T. L. Rudge, J. Mayfield, J. Schiffer, R. S. Mittler, C. C. Ibegbu, et al; AVRP Laboratory Working Group. 2012. A three-dose intramuscular injection schedule of anthrax vaccine adsorbed generates sustained humoral and cellular immune responses to protective antigen and provides long-term protection against inhalation anthrax in rhesus macaques. *Clin. Vaccine Immunol.* 19: 1730–1745.
40. Livingston, B. D., S. F. Little, A. Luxembourg, B. Ellefsen, and D. Hannaman. 2010. Comparative performance of a licensed anthrax vaccine versus electroporation based delivery of a PA encoding DNA vaccine in rhesus macaques. *Vaccine* 28: 1056–1061.
41. Ionin, B., R. J. Hopkins, B. Pleune, G. S. Sivko, F. M. Reid, K. H. Clement, T. L. Rudge, Jr., G. V. Stark, A. Innes, S. Sari, et al. 2013. Evaluation of immunogenicity and efficacy of anthrax vaccine adsorbed for postexposure prophylaxis. *Clin. Vaccine Immunol.* 20: 1016–1026.
42. Chawla, A., S. Midha, and R. Bhatnagar. 2009. Efficacy of recombinant anthrax vaccine against *Bacillus anthracis* aerosol spore challenge: preclinical evaluation in rabbits and Rhesus monkeys. *Biotechnol. J.* 4: 391–399.
43. Hopkins, R. J., N. F. Daczkowski, P. E. Kaptur, D. Muse, E. Sheldon, C. LaForce, S. Sari, T. L. Rudge, and E. Bernton. 2013. Randomized, double-blind, placebo-controlled, safety and immunogenicity study of 4 formulations of

anthrax vaccine adsorbed plus CPG 7909 (AV7909) in healthy adult volunteers. *Vaccine* 31: 3051–3058.

44. Rynkiewicz, D., M. Rathkopf, I. Sim, A. T. Waytes, R. J. Hopkins, L. Giri, D. DeMuria, J. Ransom, J. Quinn, G. S. Nabors, and C. J. Nielsen. 2011. Marked enhancement of the immune response to BioThrax (anthrax vaccine adsorbed) by the TLR9 agonist CPG 7909 in healthy volunteers. *Vaccine* 29: 6313–6320.

45. Klinman, D. M., H. Xie, S. F. Little, D. Currie, and B. E. Ivins. 2004. CpG oligonucleotides improve the protective immune response induced by the anthrax vaccination of rhesus macaques. *Vaccine* 22: 2881–2886.

46. Rao, M., K. K. Peachman, Q. Li, G. R. Matyas, S. B. Shivachandra, R. Borschel, V. I. Morthole, C. Fernandez-Prada, C. R. Alving, and V. B. Rao. 2011. Highly effective generic adjuvant systems for orphan or poverty-related vaccines. *Vaccine* 29: 873–877.

47. Malyala, P., D. T. O'Hagan, and M. Singh. 2009. Enhancing the therapeutic efficacy of CpG oligonucleotides using biodegradable microparticles. *Adv. Drug Deliv. Rev.* 61: 218–225.

48. Shivahare, R., P. Vishwakarma, N. Parmar, P. K. Yadav, W. Haq, M. Srivastava, S. Gupta, and S. Kar. 2014. Combination of liposomal CpG oligodeoxynucleotide 2006 and miltefosine induces strong cell-mediated immunity during experimental visceral leishmaniasis. *PLoS One* 9: e94596.

49. Xie, H., I. Gursel, B. E. Ivins, M. Singh, D. T. O'Hagan, J. B. Ulmer, and D. M. Klinman. 2005. CpG oligodeoxynucleotides adsorbed onto polylactide-co-glycolide microparticles improve the immunogenicity and protective activity of the licensed anthrax vaccine. *Infect. Immun.* 73: 828–833.

50. Wu, S., Z. Zhang, R. Yu, J. Zhang, Y. Liu, X. Song, S. Yi, J. Liu, J. Chen, Y. Yin, et al. 2014. Intramuscular delivery of adenovirus serotype 5 vector expressing humanized protective antigen induces rapid protection against anthrax that may bypass intranasally originated preexisting adenovirus immunity. *Clin. Vaccine Immunol.* 21: 156–164.

51. Zhang, J., E. Jex, T. Feng, G. S. Sivko, L. W. Baillie, S. Goldman, K. R. Van Kampen, and D. C. Tang. 2013. An adenovirus-vectored nasal vaccine confers rapid and sustained protection against anthrax in a single-dose regimen. *Clin. Vaccine Immunol.* 20: 1–8.

52. Feinen, B., N. Petrovsky, A. Verma, and T. J. Merkel. 2014. Advax-adjuvanted recombinant protective antigen provides protection against inhalational anthrax that is further enhanced by addition of murabutide adjuvant. *Clin. Vaccine Immunol.* 21: 580–586.

53. Schully, K. L., S. Sharma, K. J. Peine, J. Pesce, M. A. Elberson, M. E. Fonseca, A. M. Prouty, M. G. Bell, H. Borteh, M. Gallovic, et al. 2013. Rapid vaccination using an acetalated dextran microparticulate subunit vaccine confers protection against triplicate challenge by bacillus anthracis. *Pharm. Res.* 30: 1349–1361.

54. Mosier, D. E., and W. E. Paul. 1975. The role of antigen presentation in B cell activation: analysis with two DNP-Polymer conjugates. In *Immune Recognition*. A. S. Rosenthal, ed. Academic, New York, p. 133–152.

55. Mosca, F., E. Tritto, A. Muzzi, E. Monaci, F. Bagnoli, C. Iavarone, D. O'Hagan, R. Rappuoli, and E. De Gregorio. 2008. Molecular and cellular signatures of human vaccine adjuvants. *Proc. Natl. Acad. Sci. USA* 105: 10501–10506.

56. Caproni, E., E. Tritto, M. Cortese, A. Muzzi, F. Mosca, E. Monaci, B. Baudner, A. Seubert, and E. De Gregorio. 2012. MF59 and Pam3CSK4 boost adaptive responses to influenza subunit vaccine through an IFN type I-independent mechanism of action. *J. Immunol.* 188: 3088–3098.

57. Awate, S., L. A. Babiuk, and G. Mutwiri. 2013. Mechanisms of action of adjuvants. *Front. Immunol.* 4: 114.

58. Skowera, A., E. C. de Jong, J. H. Schuitemaker, J. S. Allen, S. C. Wessely, G. Griffiths, M. Kapsenberg, and M. Peakman. 2005. Analysis of anthrax and plague biowarfare vaccine interactions with human monocyte-derived dendritic cells. *J. Immunol.* 175: 7235–7243.

59. Hawiger, D., K. Inaba, Y. Dorsett, M. Guo, K. Mahnke, M. Rivera, J. V. Ravetch, R. M. Steinman, and M. C. Nussenzweig. 2001. Dendritic cells induce peripheral T cell unresponsiveness under steady state conditions in vivo. *J. Exp. Med.* 194: 769–779.

60. Krishnamachari, Y., and A. K. Salem. 2009. Innovative strategies for co-delivering antigens and CpG oligonucleotides. *Adv. Drug Deliv. Rev.* 61: 205–217.

61. Bentebibel, S. E., S. Lopez, G. Obermoser, N. Schmitt, C. Mueller, C. Harrod, E. Flano, A. Mejias, R. A. Albrecht, D. Blankenship, et al. 2013. Induction of ICOS⁺CXCR3⁺CXCR5⁺ T_H cells correlates with antibody responses to influenza vaccination. *Sci. Transl. Med.* 5: 176ra32.

62. Koyama, S., T. Aoshi, T. Tanimoto, Y. Kumagai, K. Kobiyama, T. Tougan, K. Sakurai, C. Coban, T. Horii, S. Akira, and K. J. Ishii. 2010. Plasmacytoid dendritic cells delineate immunogenicity of influenza vaccine subtypes. *Sci. Transl. Med.* 2: 25ra24.

63. Liu, H., K. D. Moynihan, Y. Zheng, G. L. Szeto, A. V. Li, B. Huang, D. S. Van Egeren, C. Park, and D. J. Irvine. 2014. Structure-based programming of lymph-node targeting in molecular vaccines. *Nature* 507: 519–522.

64. Bourquin, C., D. Anz, K. Zwiorek, A. L. Lanz, S. Fuchs, S. Weigel, C. Wurzenberger, P. von der Borch, M. Golic, S. Moder, et al. 2008. Targeting CpG oligonucleotides to the lymph node by nanoparticles elicits efficient antitumoral immunity. *J. Immunol.* 181: 2990–2998.

Supplemental Table 1. Sequence information for murine primers used in QRT-PCR analysis

Ubb	fwd	TGGCTATTAATTATTCGGTCTGCAT
	rev	GCAAGTGGCTAGAGTGCAGAGTAA
Mx1	fwd	TCTGTGCAGGCACTATGAGG
	rev	GCCTCTCCACTCCTCTCCTT
Isg15	fwd	ACGGTCTTACCCTTTCCAGTC
	rev	CCCCTTTCGTTCCTCACCAG
Irf7	fwd	ACAGGGCGTTTTATCTTGCG
	rev	TCCAAGCTCCCGGCTAAGT
Ifit	fwd	AGGCTGGAGTGTGCTGAGAT
	rev	TCTGGATTTAACCGGACAGC
Sele	fwd	CCGTCCCTTGGTAGTTGCA
	rev	CAAGTAGAGCAATGAGGACGATGT
Selp	fwd	CGTCTCAGAAAGAAAGATGATGGAA
	rev	TGGGTCATATGCAGCGTTAGTG
Lfa1a	fwd	CGTGCTCAGCGGCATTG
	rev	CAGGTACTGCCAGAGGGTCAGT
Mac1	fwd	CTCTGAGAAATGACGGTGAGGAT
	rev	CCTTCCGGTAAGATAAGCCAGAT
Mmp3	fwd	TTTAAAGGAAATCAGTTCTGGGCTATA
	rev	CGATCTTCTTCACGGTTGCA
Mmp9	fwd	CACCTTCACCCGCGTGTAC
	rev	TGCTCCGCGACACCAAA
Ifna12	QIAGEN catalog #PPM03671F	
Oas2	QIAGEN catalog #PPM35813A	

FWD = forward primer; REV = reverse
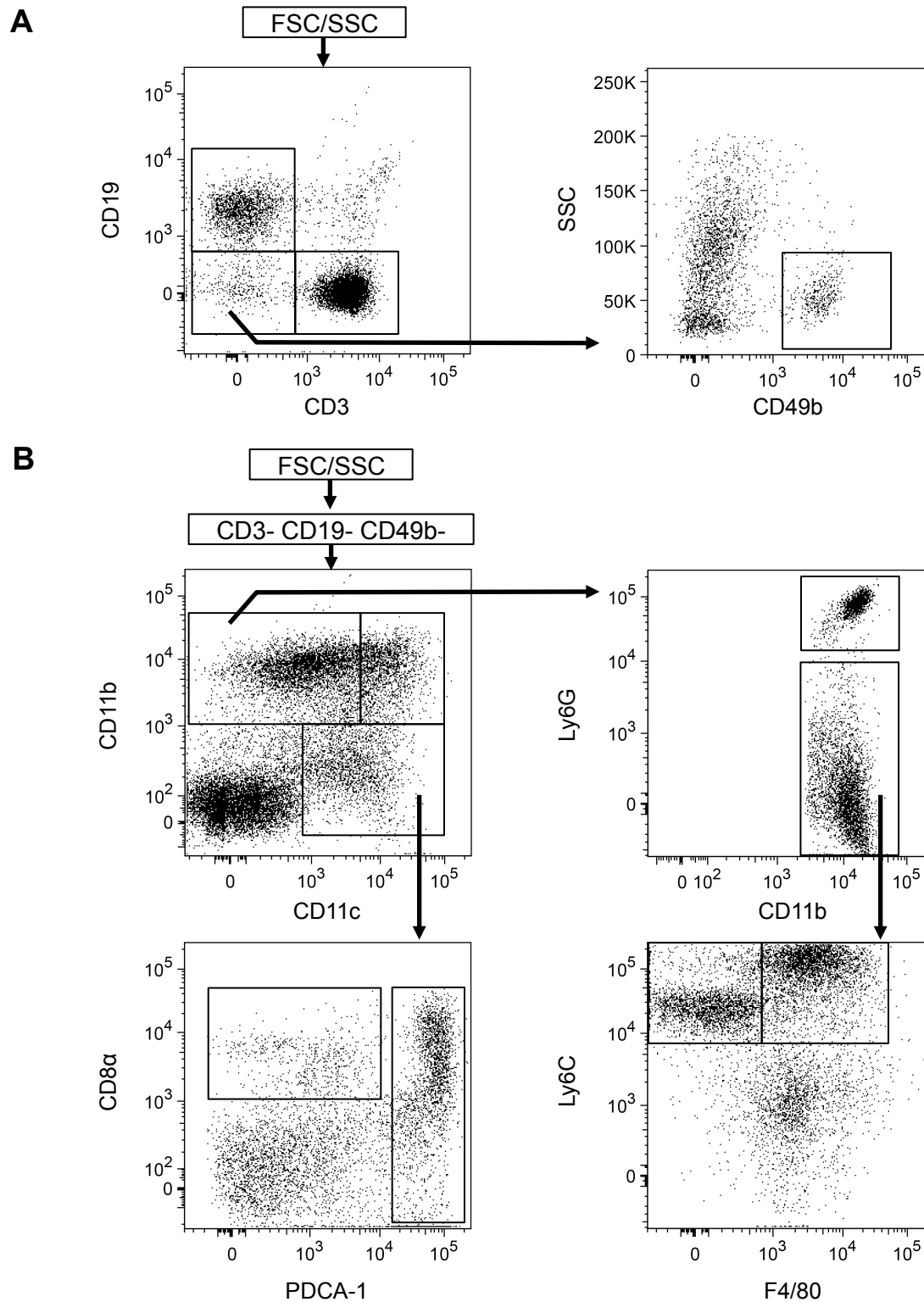
Supplemental Figure 1. Representative flow cytometry gating strategy for differentiation of cell populations. (A) Following light scatter gating, T cells were identified as $CD3^+/CD19^-$, B cells as $CD3^-/CD19^+$, and NK cells as $CD3^-/CD19^-/CD49b^+$. (B) Following light scatter gating and exclusion of lymphocytes using a dump channel, myeloid cells ($CD11b^+$) were identified as $CD11b^+/CD11c^-$, mDCs as $CD11b^+/CD11c^+$, and cDCs as $CD11b^-/CD11c^+$. pDCs were gated as $CD11b^-/CD11c^+/PDCA1^+$, and $CD8\alpha^+$ DCs as $CD11b^-/CD11c^+/CD8\alpha^+$. Neutrophils were identified as $CD11b^+/CD11c^-/Ly6G^+$, while macrophages were defined as $CD11b^+/CD11c^-/F4/80^+/Ly6C^+/Ly6G^-$, and monocytes as $CD11b^+/CD11c^-/F4/80^-/Ly6C^+/Ly6G^-$. In certain experiments, cells were additionally gated for MHC II expression as indicated in figure legends.
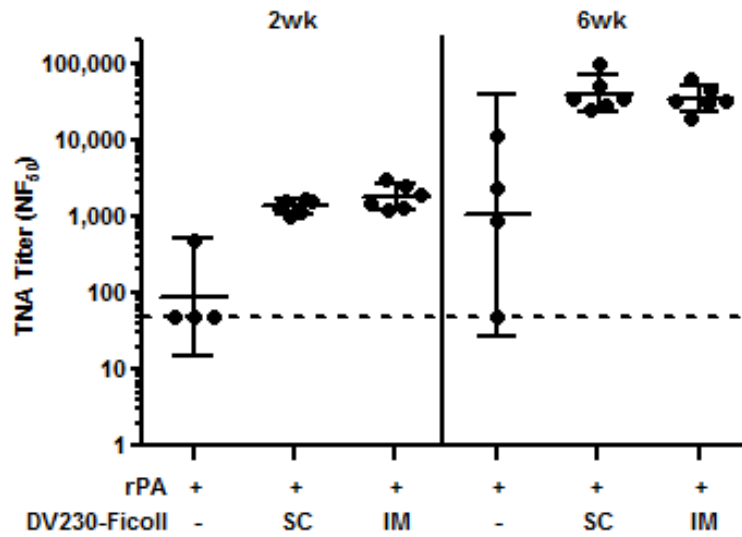
Supplemental Figure 2. Intramuscular and subcutaneous routes of immunization induce equivalent antibody response. Cynomolgus macaques (n=4-6) were immunized with 10 µg rPA alone or in combination with 1000 µg DV230-Ficoll on days 0 and 28. TNA titers levels at two and six weeks are shown as mean with 95% CI; data are from a single experiment.